4-30-2018

CREB Binding Protein Exerts Transcriptional and Post-translational Regulatory Effects on Dendritic Arborization in Drosophila Sensory Neurons

Sarah Glenn Clark
Georgia State University

CREB BINDING PROTEIN EXERTS TRANSCRIPTIONAL AND POST-TRANSLATIONAL REGULATORY EFFECTS ON DENDRITIC ARBORIZATION IN *DROSOPHILA* SENSORY NEURONS

by

SARAH CLARK

Under the Direction of Daniel N. Cox, PhD

ABSTRACT

The *Drosophila* ortholog of CREB Binding Protein (dCBP) has been implicated in the pruning of sensory neuron dendrites and recent studies demonstrate that nuclear polyglutamate-induced dendritic pathologies occur, in part, by inhibiting Golgi outpost formation via a CBP-CrebA-COPII regulatory mechanism. Despite these advances, the role of dCBP in modulating dendritic development is incompletely understood. Here, we identify dCBP as a novel regulator of dendritic development that modulates the localization of Dar1, a protein known to affect dendritic growth via regulation of the microtubule severing protein Spastin and components of the Dynein complex. We discovered that dCBP is required for proper proximal-distal branch order distribution, with loss of function resulting in an aberrant reduction in terminal branching in favor of a shift towards proximal interstitial branching. Conversely, dCBP overexpression severely inhibits higher order dendritic branching in Class IV (CIV) md sensory neurons. Detailed structure-function studies using domain-specific deletions of dCBP provide further

insights into the specific roles of different protein domains in mediating distinct aspects of dendritic growth. Analyses of domain-specific deletions implicate the N-terminal region (ΔNZK) in regulating the mutant phenotype, whereas expression of a deletion of the C-terminal region (ΔQ) phenocopies the overexpression phenotype. To characterize dCBP-mediated transcriptional mechanisms driving dendrite arborization, we conducted RNAseq analyses focusing on those genes that fail to be transcriptionally regulated by the ΔNZK deletion. These analyses reveal a primary role for dCBP in transcriptional repression. Enriched gene clusters included phosphorylation, ubiquitination, microtubule-based processes, protein modification processes, cytoskeletal organization, and cell morphogenesis. To characterize these putative regulatory targets, we simultaneously expressed the ΔNZK deletion construct in combination with gene-specific knockdown. These analyses revealed that disruptions of Arp53D, CG12620, CG31391, CG16716, and α-actinin 3 partially rescue aspects of morphological defects that are caused by expression of the ΔNZK construct. Combined with cytoskeletal imaging, our results suggest that dCBP function includes transcriptional repression of genes that may otherwise over-stabilize both actin and microtubule components thereby contributing to cytoskeletal dynamics required for dendritic growth. Collectively, these analyses identified transcriptional and post-translational regulatory mechanisms by which dCBP functions to direct the specification of distinct neuronal morphologies.

INDEX WORDS: CREB binding protein, Dendrite development, Transcription factors,
Cytoskeleton, Post-translational modification, Sensory neuron

CREB BINDING PROTEIN EXERTS TRANSCRIPTIONAL AND POST-TRANSLATIONAL REGULATORY EFFECTS ON DENDRITIC ARBORIZATION IN *DROSOPHILA* SENSORY NEURONS

by

SARAH CLARK

A Dissertation Submitted in Partial Fulfillment of the Requirements for the Degree of

Doctor of Philosophy

in the College of Arts and Sciences

Georgia State University

2018

CREB BINDING PROTEIN EXERTS TRANSCRIPTIONAL AND POST-TRANSLATIONAL REGULATORY EFFECTS ON DENDRITIC ARBORIZATION IN *DROSOPHILA* SENSORY NEURONS

by

SARAH CLARK

Committee Chair: Daniel Cox

Committee: Victor Faundez

Sarah Pallas

Marise Parent

Electronic Version Approved:

Office of Graduate Studies

College of Arts and Sciences

Georgia State University

May 2018

ACKNOWLEDGEMENTS

First I would like to thank Dr. Daniel Cox, who has been my friend and mentor throughout this journey even before I joined his lab, and without whose support and encouragement I would almost certainly have given up on graduate school at several different points.

I would also like to thank all of the members of the Cox Lab, particularly Atit Patel, Shatabdi Bhatacharjee, and Surajit Bhattacharya who were instrumental in the RNAseq project, and Myurajan Rubaharan who worked on the Dar1 project at George Mason University. Also my wonderful undergraduate assistants Joshua Lott and Ashwini Sangaraju, without whom none of this would have gotten finished, as well as Siddharth Poyapakkam and Uy Nguyen, who took time from working with Shatabdi to help me get some last-minute work finished.

Dr. Victor Faundez, Dr. Sarah Pallas, and Dr. Marise Parent for taking the time to be on my committee and for giving me valuable feedback and support, as well as Dr. Kyle Frantz and Dr. Joseph Normandin for giving me an amazing teaching opportunity and letting me learn from them.

My husband, Courtney Swanson, as well as my parents Alice and Jeff Clark and my sister Caroline Clark, without whose support I never would have survived graduate school.

Finally, I'd like to thank our collaborators in the *Drosophila* community, and both the Brains & Behavior and 2CI Neurogenomics programs at Georgia State University for their support.

TABLE OF CONTENTS

LIST OF FIGURES

1 INTRODUCTION

1.1 Dendritic development and neurological disease

Cognition and behavior emerge from circuits of neurons in the brain. Therefore, comprehension of neural architecture is a necessary step towards understanding computation in the nervous system (Chiang et al. 2011, Helmstaedter and Mitra 2012). Two distinct tree-shaped neuronal structures, differing in both structure and function, are responsible for wiring the circuitry: dendrites and axons. Dendrites receive, integrate, transform, and propagate to the soma signals from other neurons, thus largely defining the computational properties of a neuron. In contrast, axons transmit signals to other neurons, often spanning long distances to connect the network. Dendritic arbors remain plastic to a certain extent even after reaching a steady mature shape, and continuously adjust their existing structure (Lefebvre and Sanes, 2015). However, overall stability of mature dendrites is necessary for proper functioning of mature circuits and destabilizing dendritic morphology may cause neurodegeneration and functional impairment. Neuronal cell types are often defined by the morphology of their dendritic arbors (e.g. stellate cells, pyramidal cells) and defects in dendritic morphology are highly correlated with an assortment of developmental and neurological disorders. In sensory neurons, dendritic atrophy can result in an animal's failure to perceive a dangerous stimulus (Honjo et al. 2016), whereas dendritic hypertrophy could result in exaggerated responses to benign stimuli. Thus, the animal must have genetic programs in place to ensure that each neuron will achieve an appropriate level of dendritic complexity and be responsive to activity-dependent cues that allow for dendritic dynamics, such as occurs in dendritic spines during learning and memory.

Elucidating the molecular genetic mechanisms by which multiple local interactions of cytoskeleton elements direct the growth of dendrite arbors has direct clinical relevance because

disrupted arbor development is a common feature in a diverse variety of neuropathological disease states, including Down, Rett, and Fragile X Syndromes; autism; Alzheimer's, Parkinson's, and Huntington's diseases; schizophrenia, and Duchenne/Becker muscular dystrophies (Belmonte et al. 2004, Anderton et al. 1998, Sheetz et al. 1998, Dickson et al. 1999, Jagadha and Becker 1988, Fiala et al. 2002, Kaufmann and Moser 2000, Ramocki and Zoghbi 2008, Kulkarni and Firestein 2012), in all of which strong neuroanatomical correlations exist between dendritic abnormalities and cognitive impairments. Learning to manipulate arbor growth mechanisms will be important to the development of neuro-regenerative strategies. Dendrites are the chief site of signal input into a neuron, receiving up to tens of thousands of inputs on each arbor. In addition, correct dendrite arbor and spine morphologies are central to the proper establishment of synapses, and in turn, neuronal circuits. Thus, achieving an understanding of the regulatory mechanisms governing dendritic development will aid in understanding the cellular and molecular bases of pathologies underlying human neurological disease.

1.2 *Drosophila melanogaster* as a model system for elucidating molecular control of dendritogenesis

Research in *Drosophila* has yielded significant insight into the cellular and molecular processes driving cell-type specific dendritogenesis and neural circuit construction (Jan and Jan 2010, Santiago and Bashaw 2014, Couton et al. 2015, Lefebvre et al. 2015, Nanda et al. 2017). Here, we focus on one of the most widely studied models for investigating dendritic development in the fruit fly, namely the multidendritic (md) sensory neurons of the peripheral nervous system. *Drosophila* md neurons constitute an attractive model to investigate the

molecular mechanisms underlying the regulation of dendritic morphology and sensory behavior for several reasons: 1) powerful genetic tools are available in the fruit fly for investigating gene function; 2) the dendritic arbor lies immediately below a translucent, thin larval epithelium facilitating *in vivo* live cell and time-lapse imaging; 3) the class-specific diversity in tree morphology within this group of neurons facilitates comparative analyses of the key elements controlling the acquisition and maintenance of cell-type specific dendritic arborization and the promotion of dendritic diversity; and 4) distinct md neuron subclasses regulate a range of somatosensory behaviors, facilitating analyses of dendritic form and function. Morphological phenomena including dendritic growth, branching, scaling, tiling, and remodeling have all been characterized using md neurons (reviewed in Jan and Jan 2010, Singhania and Grueber 2014, Tavosanis 2014, Nanda et al. 2017). These md neurons are grouped into four distinct morphological classes (Class I-IV) based on increasing complexity of their dendritic arbors

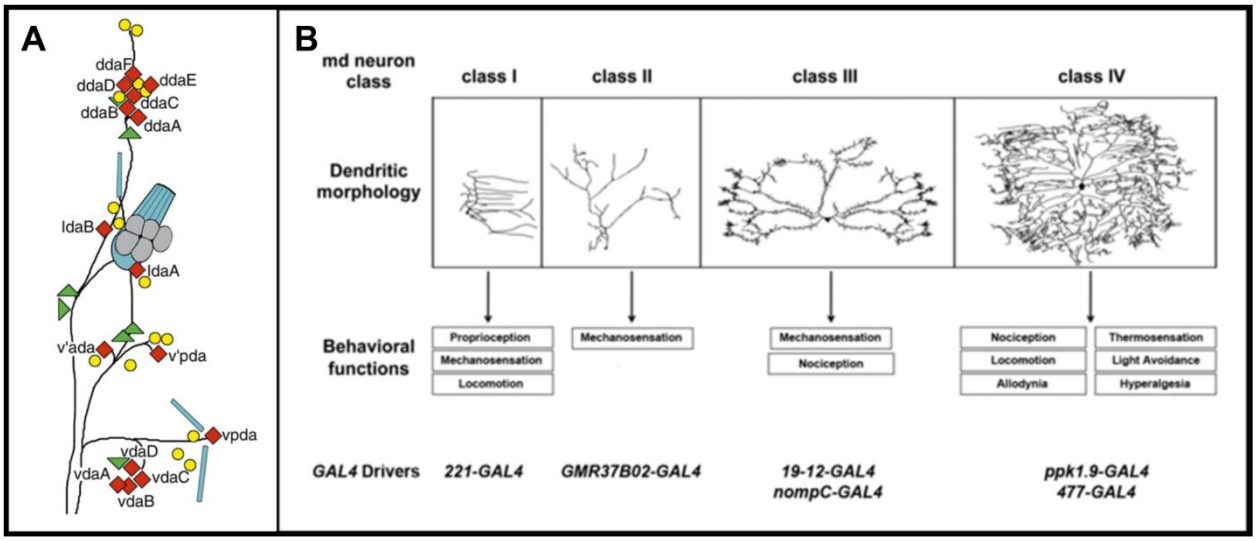

Figure 1.1 Drosophila md sensory neurons.
(Grueber et al. 2002) (**Fig. 1.1**).

(A) Schematic of the distribution of PNS sensory neurons for an individual hemisegment; type I mono-dendritic neurons include external sensory neurons (yellow circles) and chordotonal stretch receptor neurons (teal bars); type II multidendritic (md) sensory neurons include bipolar

neurons and tracheal dendrite neurons (green triangles) as well as md sensory neurons (class I-IV) (red diamonds). (B) Representative images of md neuron dendritic morphologies by class, together with known behavioral functions and GAL4 drivers that mediate class-specific expression. Panel (A) adapted from Grueber et al. (2002). Panel (B) adapted from Turner et al. (2016).

Studies over the past fifteen years have revealed numerous genetic and cellular programs that govern cell type-specific dendrite development including transcriptional regulation, intrinsic and extrinsic cell signaling pathways, secretory and endocytic pathway function, cytoskeletal modulation, cell adhesion, RNA targeting and local translation, chromatin remodeling, and activity-dependent modulation of dendritic arborization. Moreover, approximately half of the proteins produced by the fly genome have mammalian homologs and three-fourths of known human disease genes have a *Drosophila* ortholog (Reiter et al. 2001). The ease with which specific mutations can be generated and tracked makes *Drosophila* an efficient and effective model for many human diseases and disorders, including Parkinson's disease, Huntington's disease, Alzheimer's disease, seizure disorders, sleep disturbances, and mental retardation (Bellen et al. 2010).

1.3 Transcriptional regulation of dendritic morphology

Cell type-specific dendritic morphologies emerge via complex growth mechanisms modulated by intrinsic signaling involving transcription factors (TFs) that mediate neuronal identity as well as functional and morphological properties of the neuron subtype (Jan and Jan 2010; Lefebvre et al. 2015; Nanda et al. 2017). Moreover, dendrite development is modulated by extrinsic signaling, influenced by external factors such as peripheral glial cells (Yamamoto et al. 2006), and coupled with activity-dependent regulation (Jan and Jan 2010; Tavosanis 2014). Combined, these processes converge on a broad spectrum of cellular pathways, including

pathways that regulate the cytoskeleton, to direct cell type-specific dendritic arbor development, stabilize mature architecture, and facilitate structural plasticity.

TFs have been demonstrated to exert their effects on dendrite morphogenesis by several different mechanisms. TFs are used by neurons to fine-tune the level of expression of many genes. Distinct cell fates and morphologies can be achieved by the presence or absence of a TF, by varying the levels of an individual TF, or by a combinatorial mechanism of action that can involve many TFs (Santiago and Bashaw 2014, Puram and Bonni 2013, Jan and Jan 2010) (**Fig. 1.2 B**). Transcriptional control facilitates fine-tuning of gene expression levels, which ultimately contributes to the protein complement that an individual neuronal subtype expresses, thereby dictating neuronal form and function. Furthermore, recent evidence reveals that TFs involved in cell fate specification may also exhibit independent post-mitotic roles in directing cell-type specific neural differentiation, *e.g.* dendrite morphogenesis (Iyer et al. 2013a, de la Torre-Ubieta and Bonni 2011).

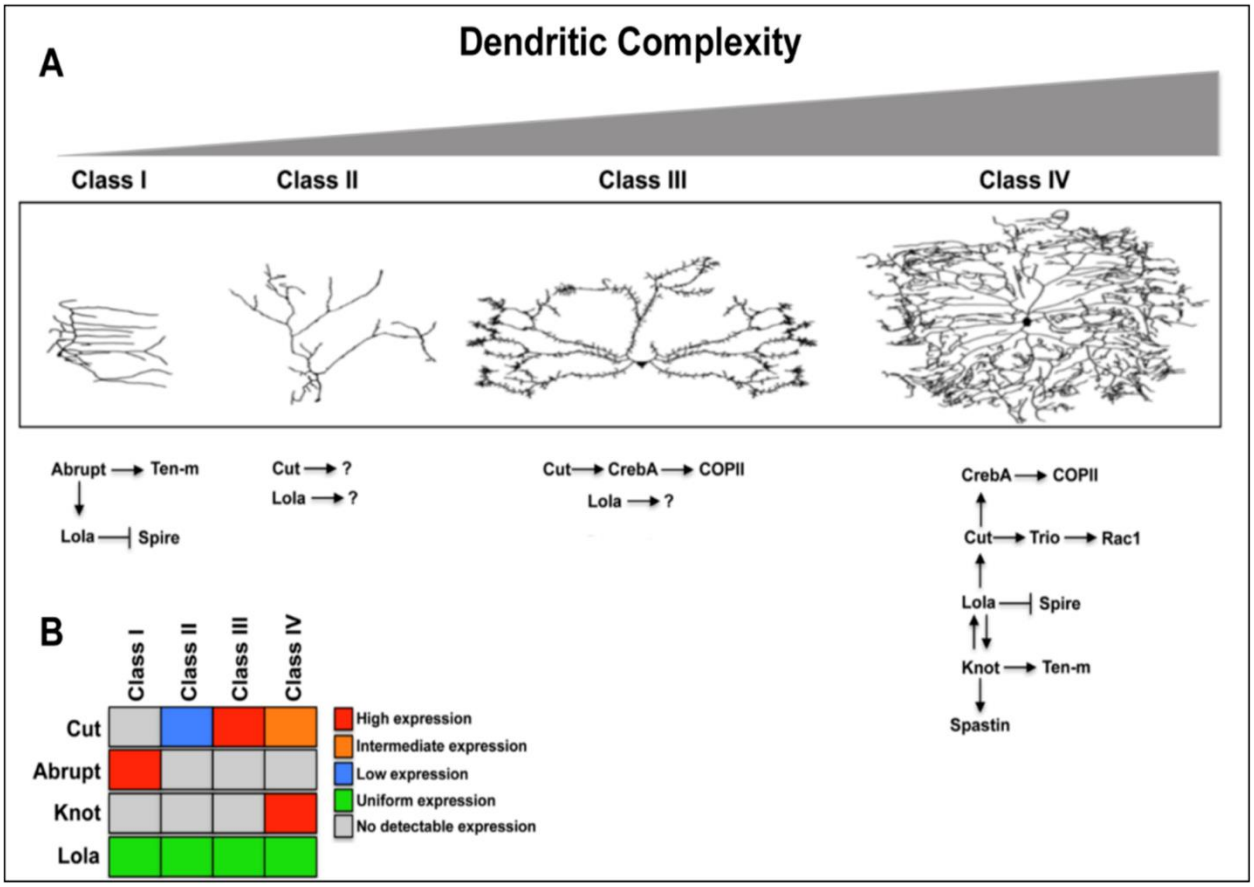

Figure 1.2 Transcriptional regulation of md sensory neuron dendritic architecture.

(A) Shown at top are representative tracings of dendritic architecture among class I-IV Drosophila md sensory neurons. Shown below are known transcriptional regulatory programs that operate in individual md neuron subclasses to mediate class-specific dendritogenesis. Arrows indicate transcriptional activation, whereas bars represent transcriptional repression. (B) Summary of transcription factor protein expression levels and differential expression by da neuron subclass. Adapted from Nanda et al. (2017).

Comprehensive studies in *Drosophila* md sensory neurons have provided substantial insight into individual and combinatorial roles for TFs in driving class-specific dendritogenesis (Hattori et al. 2007, Jinushi-Nakao et al. 2007, Kim et al. 2006, Moore et al. 2002, Sugimura et al. 2004, Sulkowski et al. 2011, Ye et al. 2011, Grueber et al. 2003, Crozatier and Vincent 2008, Li et al. 2004, Iyer et al. 2013a, Iyer et al. 2013b, Das et al. 2017), however the molecular

mechanisms by which these TFs govern arbor development and dynamics remains incompletely understood (Santiago and Bashaw 2014). An ensemble of TFs, including Cut, Abrupt, Knot (also known as Collier), and Lola (**Fig. 1.2**), are required as major regulators of cell type-specific md sensory neuron dendritic morphogenesis, and although recent studies have begun to link cell type-specific TF activity to cytoskeletal regulation and other pathways (Ferreira et al. 2014, Hattori et al. 2013, Iyer et al. 2012, Iyer et al. 2013b, Jinushi-Nakao et al. 2007, Nagel et al. 2012, Ye et al. 2011, Das et al. 2017), much remains unknown regarding the molecular mechanisms by which TFs direct final arbor shape. A summary of the current state of knowledge regarding the expressivity and mechanisms by which these TFs regulate differential patterns of dendrite arborization is depicted in **Fig. 1.2 A**.

TF regulation of dendritic morphology is not unique to *Drosophila*, but rather is a conserved mechanism observed across metazoans from *C. elegans* to *H. sapiens*. For example, Neurogenin 2 has a crucial role in the specification of dendrite morphology of pyramidal neurons in the neocortex: it promotes the outgrowth of a polarized leading process during the initiation of radial migration (Hand et al. 2005). Studies in *C. elegans* have revealed that UNC-86 controls dendritic outgrowth and cell identity in PVD nociceptive sensory neurons (Smith et al. 2010). Furthermore, in the zebrafish Rohon-Beard (RB) spinal sensory neurons, the LIM homeodomain transcription factor regulates the ability of microtubules to invade filopodia and mediates interactions between the microtubule and actin cytoskeleton, thus affecting several cell motility processes during RB morphogenesis (Andersen et al. 2011).

1.4 Post-translational regulation of dendritic morphology

Beyond transcriptional regulation of gene expression, gene product activity can also be modulated indirectly by activation or inactivation of the protein product via post-translational modifications or by changes in subcellular localization. For example, the homeodomain transcription factor Cut normally is not expressed in class I md neurons. Ectopic expression of Cut leads to a conversion of dendritic morphology such that the arbor takes on morphological characteristics of class III md neurons, which normally express Cut at high levels (Grueber et al., 2003). Protein-protein interactions have likewise been shown to regulate dendritic architecture (*e.g.* dendritic spines). Many neuronal proteins are in a state of near-constant flux, undergoing different post-translational modifications and associating and disassociating with other proteins in order to carry out the many tasks required for healthy neuronal functioning. For example, the protein spinophilin is known to bind directly to and stabilize actin filaments in a manner dependent upon its phosphorylation state (Feng et al. 2000). Additionally, spinophilin binds directly to protein phosphatase-1, which has been shown to dephosphorylate actin filaments (Feng et al. 2000). Thus, a single protein can function either to stabilize or destabilize the dendritic actin cytoskeleton depending upon its interactions with other proteins.

1.5 Mammalian CREB binding protein

CREB binding protein (CBP) is a large multi-domain protein (265 kDa) that is highly conserved across species. Mutations in CBP in humans have been causally linked to the development of Rubinstein-Taybi syndrome (Kumar et al. 2004), a rare autosomal dominant disorder that manifests with moderate to severe forms of intellectual disability (Petrij et al. 1995). CBP contains a nuclear hormone receptor (NHR) binding domain, a KIX domain (where

CREB binds), a bromodomain (which binds to acetylated lysine residues), four zinc finger domains, a histone acetyltransferase (HAT) domain, and a glutamine-rich domain. The CBP HAT domain functions in epigenetic modification via acetylation of histones and other proteins, is capable of auto-acetylation, and has been linked to neurogenesis (Chatterjee et al. 2013). The NHR domain binds to nuclear hormone receptors and promotes CBP function as an integrator of multiple signal transduction pathways within the nucleus (Kamei et al. 1996), whereas the zinc finger protein domains function in DNA recognition, lipid binding, and transcriptional activation/regulation (Laity et al. 2001).

CBP has been shown to interact with well over 70 other proteins, including many other transcription factors, *e.g.* cAMP response element binding protein (CREB) (reviewed in Vo and Goodman 2001). CBP functions as a transcriptional co-regulator of RNA polymerase II-mediated gene expression, thus integrating transcriptional responses via a variety of signal transduction pathways including Wnt and NF-κB (Li et al. 2007, Mukherjee et al. 2013) (**Fig. 1.3**).

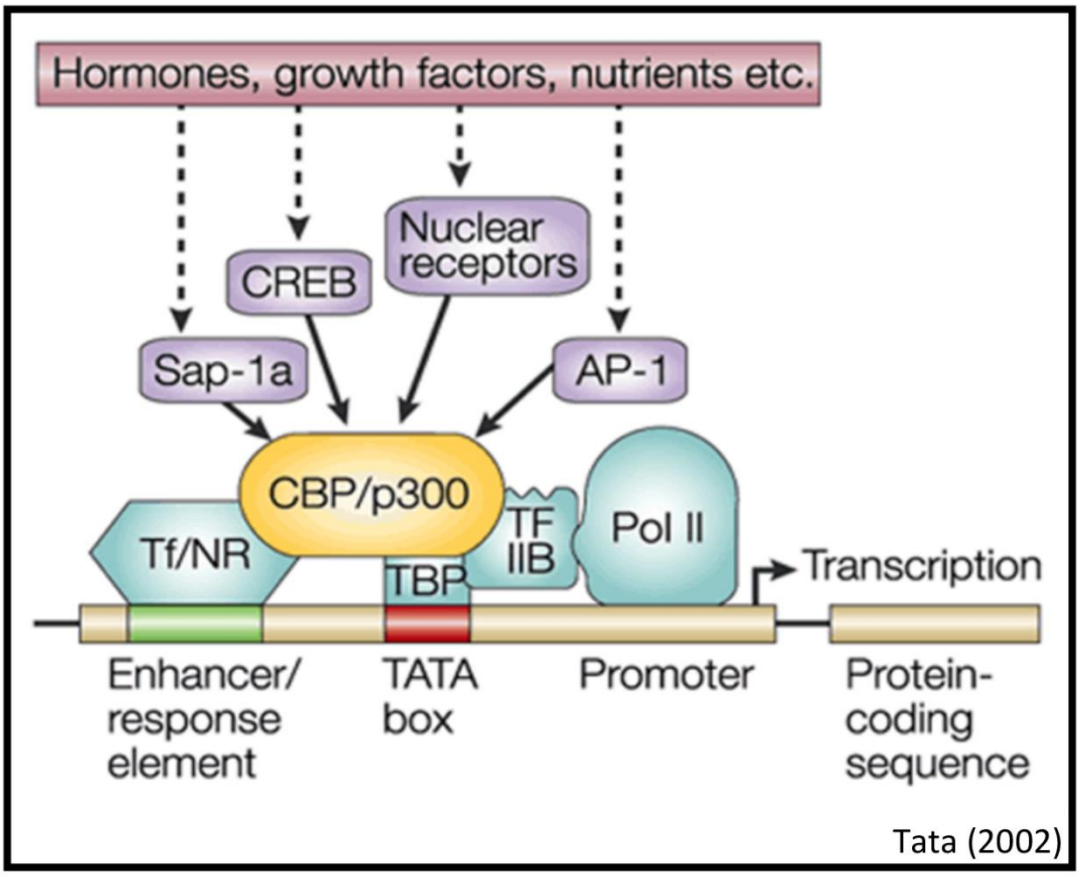

Figure 1.3 Mammalian CREB binding protein.

Depiction of a CBP-containing complex involved in RNA Polymerase II-catalyzed transcription (from Tata 2002).

CBP was originally isolated and described as a nuclear protein that binds to CREB to facilitate cAMP-regulated gene expression (Chrivia et al. 1993), but many other functions have since been described. Phosphorylation of CREB recruits CBP or its paralog p300, thereby increasing CREB transcriptional activity (Cortés-Mendoza et al. 2013). CBP has been implicated in the maintenance of circadian rhythms, the proliferation and survival of cancer cells, axon growth and regeneration, and adult neurogenesis. It is a requisite coactivator for the transcriptional activation of genes responsible for circadian rhythms, and its abnormal

degradation has in fact been implicated in the disruption of circadian rhythms that occur in Alzheimer's disease (Song et al. 2015). CBP is expressed at abnormally high levels in many types of cancerous tumors, and drug-mediated inhibition of CBP's HAT activity has been shown to inhibit cancer cell proliferation (Tang et al. 2016). CBP, along with p53, regulates the expression of GAP-43 and is thereby necessary for axon outgrowth (Tedeschi et al. 2009), and pharmacological activation of CBP has been shown to promote adult neurogenesis and increase the duration of spatial memory retention (Chatterjee et al. 2013).

In vertebrates, CREB is associated with controlling neuronal activity-dependent dendritic development (Wayman et al. 2006, Redmond et al. 2002). Moreover, CBP has also been shown to be directly involved in dendritic growth. Redmond et al. (2002) showed that calcium-dependent dendritic growth required CBP function and that direct inhibition of CBP caused greater deficits than inhibition of CREB, implying that CBP has functions in dendritic growth that go beyond its role as a CREB-mediated transcriptional co-activator. Other CBP-interacting proteins may be critical to this type of dendritic growth modulation, such as CREST (calcium-responsive transactivator). CREST is a calcium-activated transcriptional regulator that cannot bind to DNA directly, but regulates dendritic development through its interaction with CBP (Aizawa et al. 2004). In addition, CREST physically associates with the neuron-specific BRG1-associated factor (nBAF) complex, a chromatin remodeling complex involved in specification of distinct neuronal subclasses from neural progenitors (Wu et al. 2007).

1.6 *nejire* encodes the *Drosophila* ortholog of CREB binding protein (dCBP)

The *Drosophila* ortholog of CBP (dCBP) is encoded by the *nejire* gene. *Drosophila* genes are traditionally named for the phenotype that occurs with loss of function of the gene, and

nejire (*nej*) (Japanese for "twisted") was originally identified as a patterning gene whose mutation gave embryos a twisted appearance (Akimaru et al. 1997). *Nejire* encodes a 340 kDa protein that is considerably larger than mammalian CBP. Overall, the two proteins exhibit approximately 33% homology but their functional domains are all evolutionarily conserved. Like mammalian CBP, dCBP also contains NHR, KIX, bromo, HAT and glutamine-rich domains, as well as four zinc finger domains. Notably, dCBP also contains a large number of polyglutamine (poly-Q) tracts spread throughout its structure, while in mammalian CBP there is only a single poly-Q tract near the C-terminus (**Fig. 1.4**). Poly-Q tracts are involved in stabilizing protein-protein interactions (Schaefer et al. 2012), as well as transcriptional transactivation (Gemayel et al. 2015), thus it is possible that the expanded occurrence of poly-Q tracts exhibited by dCBP has a functionally important role in mediating protein-protein interactions with different regions of the molecule contributing to cell type functional specificity. The various domains of dCBP are each implicated in playing important roles in signaling and transcription, however their respective functional roles in regulating dendrite morphology remain poorly understood.

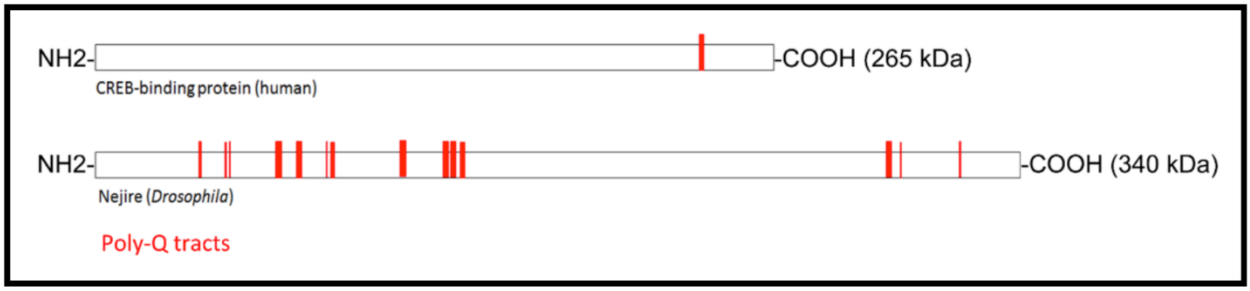

Figure 1.4 CBP and dCBP poly-Q tracts.
Schematic of human and Drosophila CBP proteins. Red sections indicate the approximate size and positions of poly-glutamine (poly-Q) tracts.

While little is known regarding the roles of dCBP in dendritic morphogenesis, a recent study has demonstrated that it plays an essential role in pruning sensory neuron dendrites during

late-stage *Drosophila* metamorphosis. During late larval stages a steroid hormone, ecdysone, starts a cascade that results in the complete collapse of md sensory neuron dendritic arbors. The Class IV and Class I md neurons then re-elaborate their dendritic arbors as part of the adult sensory nervous system, while the Class II and Class III neurons undergo apoptosis (Williams and Truman 2005). dCBP is required to activate an early-response gene in the ecdysone cascade, *sox14*, and without dCBP function dendrite pruning at the pupal stage does not occur (Kirilly et al. 2011).

1.7 Summary

The establishment and maintenance of complex dendritic arbors is of crucial importance to the proper function and survival of individual neurons, as well as the formation and modulation of neural connectivity. Numerous genes and cellular processes have been shown to play significant roles in dendritic development and it has been established that the dosage of many of these genes must be kept within a physiologically optimal range (reviewed in Copf 2015). Transcriptional regulation has emerged as a key cell intrinsic mechanism governing cell-type specific dendritic development, however the molecular mechanisms by which transcription factors regulate this process remain largely unknown. This dissertation aims to advance our understanding of regulatory processes driving dendritic development by dissecting the molecular mechanisms by which dCBP/Nejire, the *Drosophila* ortholog of CREB binding protein (CBP), acts as an essential regulator of dendritic morphology via its action as a transcriptional co-activator and through protein-protein interactions. We have identified dCBP as an essential regulator of the subcellular localization of Dar1 in CIV md neurons in later larval stages and characterized the effects of knockdown and overexpression of dCBP as well as the expression of

various dCBP structure-function mutants on the localization of Dar1 as well as their effects on dendritic morphology. Furthermore, we have utilized cell type-specific RNA sequencing combined with a phenotypic suppression screen to identify a number of putative transcriptional targets of dCBP that influence dendritic morphology and characterized the ways in which these targets might alter the morphological characteristics of CIV md neurons via cytoskeletal regulation. Taken together, these analyses reveal that dCBP executes multiple functions including utilizing transcriptional and post-translational mechanisms to direct dendritic development. In addition to expanding our understanding of molecular control of dendrite morphogenesis, the identification and characterization of downstream targets of dCBP-mediated regulation of dendritic morphology may inform future therapeutic intervention strategies designed to target CBP-mediated disease etiologies.

2 DCBP IS REQUIRED FOR SENSORY NEURON DENDRITIC DEVELOPMENT AND REGULATES THE SUBCELLULAR LOCALIZATION OF THE TRANSCRIPTION FACTOR DAR1

2.1 Scientific Premise

Genetic and molecular studies have demonstrated that the acquisition of cell-type specific dendritic morphologies is subject to regulation by complex programs involving intrinsic factors and extrinsic cues (Jan and Jan 2010, Lefebvre et al. 2015). Many of these factors are part of or activate signaling pathways that converge on transcription factors, which modulate gene expression to support both growth and dynamics of dendritic development. Among the key targets of transcriptional regulation are cytoskeletal effector molecules, which modulate cell type-specific dendritic architectures by regulating the assembly, disassembly, and reorganization of the actin and microtubule (MT) based cytoskeletons. These cytoskeletal elements form the scaffold around which cell shape is built and the tracks along which intracellular components are transported (Rodriguez et al. 2003). While class-specific TF activity has been linked to cytoskeletal regulation (Jinushi-Nakao et al. 2007, Iyer et al. 2012, Ye et al. 2011, Nagel et al. 2012, Das et al. 2017), much remains unknown regarding the molecular mechanisms by which TFs direct final arbor shape through spatio-temporal modulation of cytoskeletal dynamics, as well as other key cellular processes such as the secretory pathway and cellular signaling pathways (Santiago and Bashaw 2014).

We conducted a neurogenomic analysis of CIV md neurons coupled with a functional genetic screen to identify potential transcription factors that exert control on class-specific dendrite morphogenesis (Iyer et al. 2013a, Cox Lab, unpublished results). From this screen, we identified *CG12029* as a key mediator of CIV dendrite development. While we were conducting

detailed analyses of this gene, another study was published by Ye et al. (2011) that identified the same gene and named it *dar1* (*dendritic arbor reduction 1*). This study reported that *dar1* mutants displayed severe defects in dendritic, but not axonal growth, and that *dar1* encodes a Krüppel-like transcription factor corresponding to *CG12029*. Consistent with this study, we observed haploinsufficiency phenotypes for $dar1^{D6}$ heterozygotes and even more severe cell autonomous deficits in dendrite development of $dar1^{D6}$ homozygous mutant CIV neurons (**Fig. 2.1**).

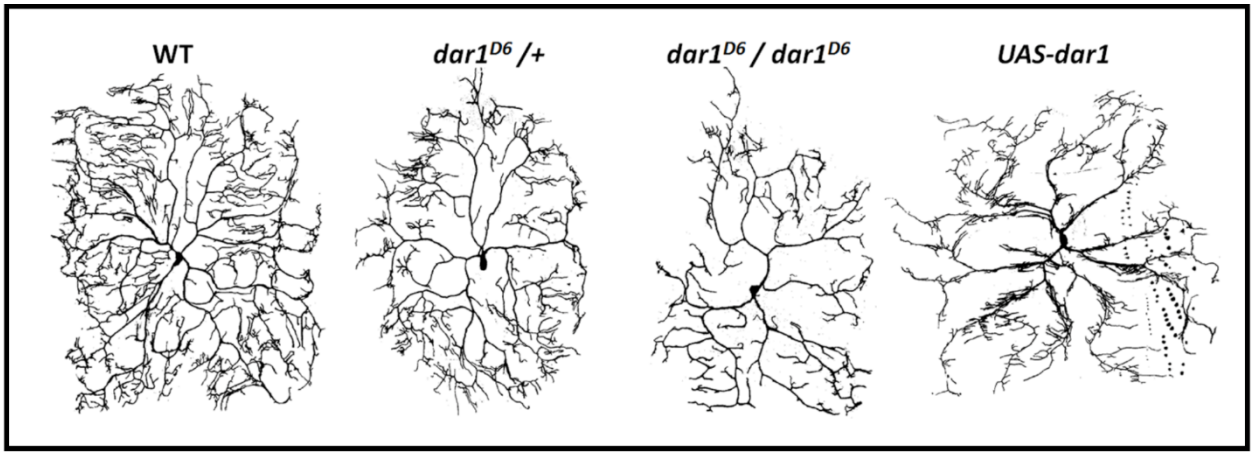

Figure 2.1 Dar1 mutation and overexpression phenotypes.
Dar1 is required to promote CIV dendritic complexity, which is sensitive to the absolute levels of Dar1 protein expression.

The study by Ye et al. (2011) asserts that Dar1 regulates dendritic development by suppressing the expression of the microtubule-severing protein Spastin, indicative of a role in mediating microtubule-based dendritic growth as no defects were observed in actin-based dendritic structures. Limitations of the previous study include that the analyses presented treat embryonic and larval data interchangeably, and the study does not examine factors other than Spastin that may be involved in Dar1-mediated dendritogenesis. Moreover, using independently developed Dar1 full-length overexpression transgenes and polyclonal antibodies, we discovered clear differences from what was previously published, in part due to the focus on embryonic

development in Ye et al. (2011). Interestingly, we observed that Dar1 overexpression in CIV neurons causes a change in branching morphology from controls with an increase in short interstitial branches, but a loss of the more complex, higher order branching typical of CIV neurons (**Fig. 2.1**).

These findings are in sharp contrast to the previous study reporting that Dar1 overexpression led to dendritic overgrowth in CIV neurons (Ye et al. 2011). In both studies, a full length Dar1 cDNA was cloned into a pUAST vector and independent transformant lines were produced. As such, the basis for the phenotypic differences observed between studies with respect to dendritic development upon Dar1 overexpression are unclear, but could potentially be due to position effect variegation which can impact the level of expressivity for different *UAS-dar1* transgene insertions. With respect to Dar1 protein expression, the study by Ye et al. (2011) reported that Dar1 is localized to the nucleus "in all cells that express Dar1", however the data upon which this assertion is based was collected exclusively from late-stage embryos. Consistent with the previous study, IHC analyses revealed that Dar1 is localized to the nucleus of all md neuron subclasses at the late embryonic stage of development (Ye et al. 2011, Cox Lab, unpublished results). However, as development proceeds to the third instar larval stage Dar1 protein is differentially localized, remaining primarily nuclear in class I-III neurons but shifting to a largely cytoplasmic localization in the highly complex CIV neurons, indicative of a cell type-dependent localization pattern **(Fig. 2.2 A)**. We confirmed the specificity of the Dar1 antibody by staining $dar1^{f01014}$ mutants which revealed virtually no detectable immunostaining **(Fig. 2.2 B)**. These distinct discoveries suggest that the localization of Dar1 may play an important functional role in mediating class-specific dendritogenesis and promoting dendritic diversity, however it is unknown how this differential subcellular localization may be regulated.

Therefore, we sought to investigate the molecular mechanisms underlying this cell type-dependent Dar1 localization by conducting an RNAi-based knockdown screen of putative Dar1-interacting molecules at the third instar larval stage. From this pilot screen we identified several putative interactors that disrupt dendritic morphology in similar ways to *dar1* mutants as well as alter the subcellular localization of Dar1 in CIV neurons. One of these putative interactors was dCBP, which we chose to investigate in more depth based on evidence from the vertebrate literature where the Dar1 ortholog, known as Krüppel-like factor 5 (KLF5), has been demonstrated to physically interact with the dCBP ortholog CBP in order to enhance KLF5 transactivation function (Zhang and Teng 2003).

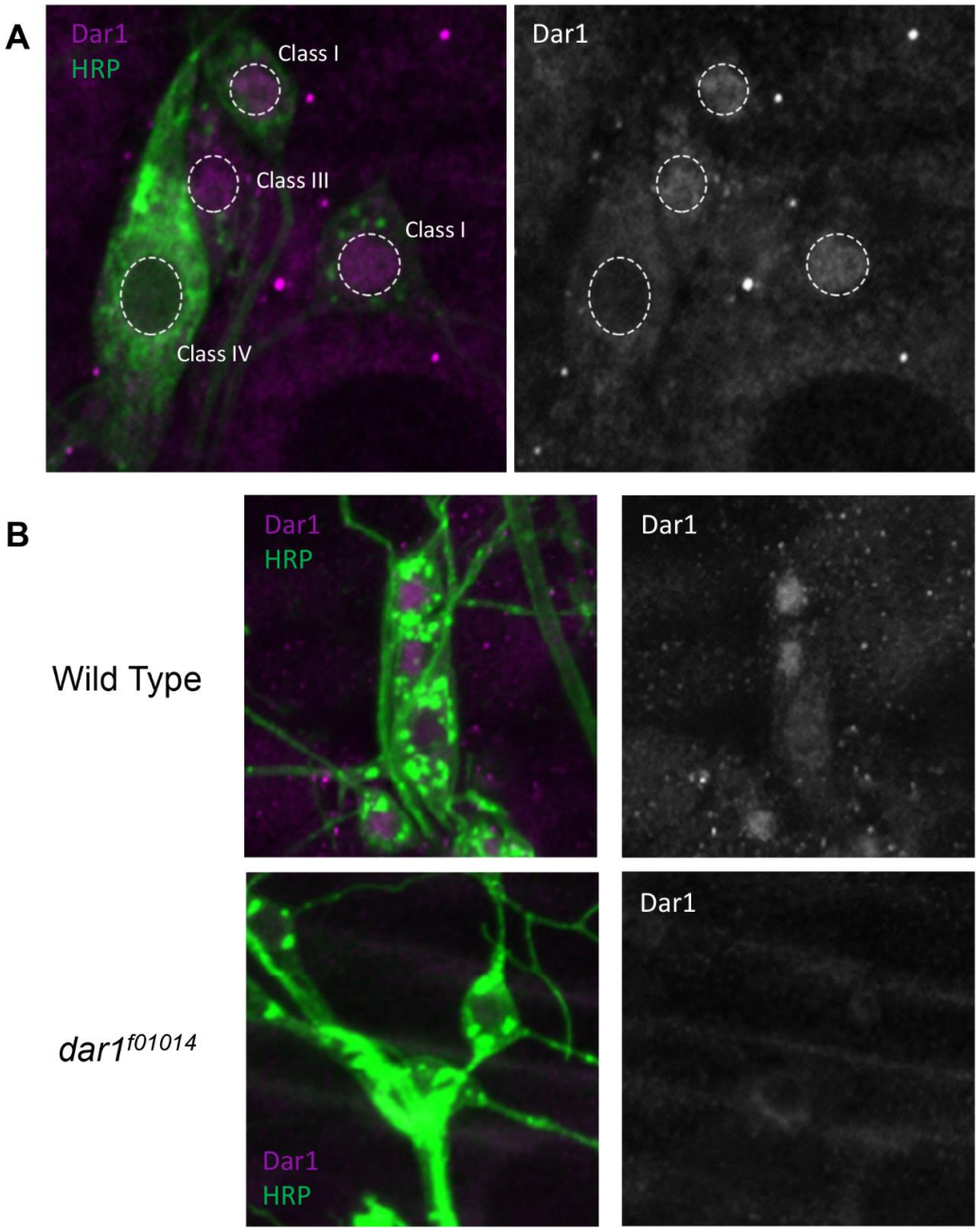

Figure 2.2 Dar1 immunostaining in WT and mutant larvae.
(A) In third instar larvae, Dar1 remains highly nuclear in Class I-III md neurons but shifts to a more cytoplasmic localization in Class IV md neurons. (B) Severely reduced immunostaining in *dar1*^{f01014} mutant larvae demonstrates antibody specificity.

2.2 Results

2.2.1 dCBP regulates dendritic growth and branching complexity

To characterize the potential roles of dCBP in regulating dendritogenesis, we conducted phenotypic analyses of *dCBP* loss-of-function (LOF) and gain-of-function (GOF) in CIV md neurons. LOF studies include *dCBP* RNAi knockdown, while GOF studies include class-specific full-length overexpression of *dCBP*. CIV-specific RNAi knockdown for *dCBP* results in a phenotype that is markedly similar to the Dar1 overexpression phenotype (**Fig. 2.1**), characterized by a shift in morphology favoring clustered interstitial dendritic branching and stripped dendritic terminals, leading to an overall reduction in the total dendritic length ($p<0.0001$), the number of terminal branches ($p=0.0001$), and the total number of branches ($p<0.0001$) (**Fig. 2.3 B, D-F**). The efficacy of the $dCBP^{RNAi}$ was confirmed by IHC analyses of dCBP protein expression following CIV-specific knockdown revealing a clear reduction in protein levels (**Fig. 2.3 B (inset), G**), while overexpression results in a notable increase in dCBP protein levels (**Fig. 2.3 C (inset), G**). In contrast to the dendritic phenotype observed with $dCBP^{RNAi}$, CIV-specific dCBP overexpression causes a loss of most higher order branches (**Fig. 2.3 C, E, H**). Notably, neither of these changes to *dCBP* expression cause any significant changes to the number of first through fourth order branches (**Fig. 2.3 B, C, H**) (see **Table S2** for specific p-values). Collectively, these analyses demonstrate that CIV dendritic development is sensitive to absolute dCBP protein levels.

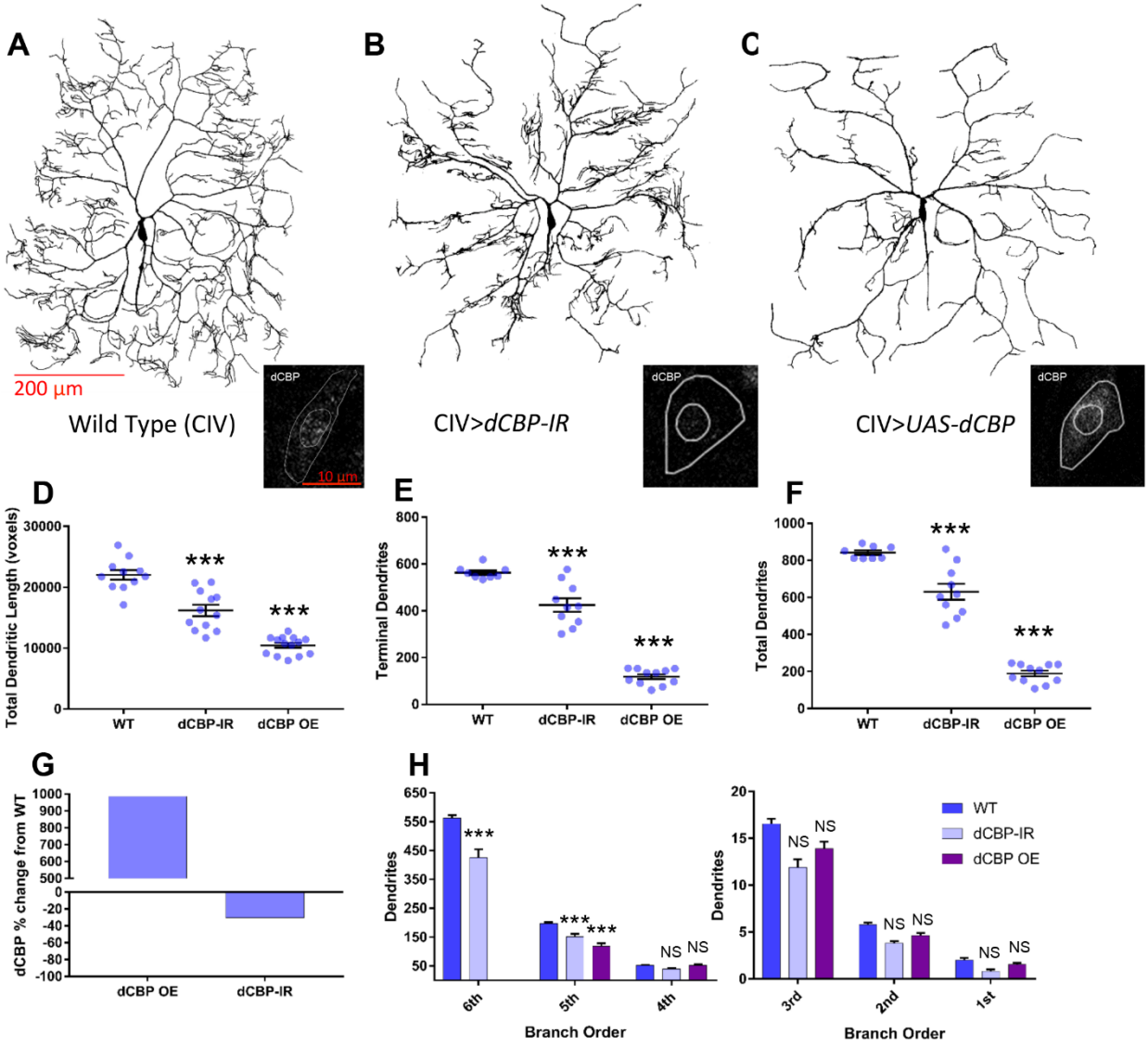

Figure 2.3 dCBP regulates dendritic growth and branching complexity.
CIV-specific phenotypic comparisons of dCBP-IR and dCBP overexpression. Insets in (A-C) show dCBP protein expression pattern. (D-F) Quantitative morphometric analyses. (G) Quantification of dCBP protein signal percent change from WT in dCBP-IR and dCBP overexpression. (H, I) Quantification of branch orders (dCBP overexpression does not reach 6th order dendrites). ***=p<0.001; NS=not significant.

2.2.2 dCBP and Dar1 exhibit differential cell type-specific subcellular localization in md neuron classes

To explore the potential interaction of dCBP and Dar1, we used LOF and GOF genetic analyses via RNAi and overexpression of full-length proteins for both dCBP and Dar1. We made

comparisons between Class I and IV md neurons using neurometric analyses to quantify and describe changes in dendritic complexity and patterns, as well as IHC analyses to quantify and describe changes in the amounts and subcellular distribution of one protein in response to disruption of the normal expression of the other. We found that there are substantial differences in subcellular localization of Dar1 between CI and CIV md neurons at the third instar larval stage **(Fig. 2.4 C, F, J)**, in contrast to previous reports (Ye et al. 2011). We established that in the morphologically simple CI neurons Dar1 is highly localized to the nucleus **(Fig. 2.4 C, J)** in comparison to the morphologically complex CIV neurons ($p<0.0001$), which show more cytoplasmic localization **(Fig. 2.4 F, J)**. dCBP follows a similar pattern of localization, with a larger proportion of the protein localized to the nucleus in the CI neurons **(Fig. 2.4 B, E, I)** ($p<0.0001$), however dCBP is also differentially expressed, with stronger expression in CI neurons relative to CIV (**Fig. 2.4 G**) ($p=0.0002$) while Dar1 is expressed at similar levels between the two classes **(Fig. 2.4 H)** ($p=0.6586$).

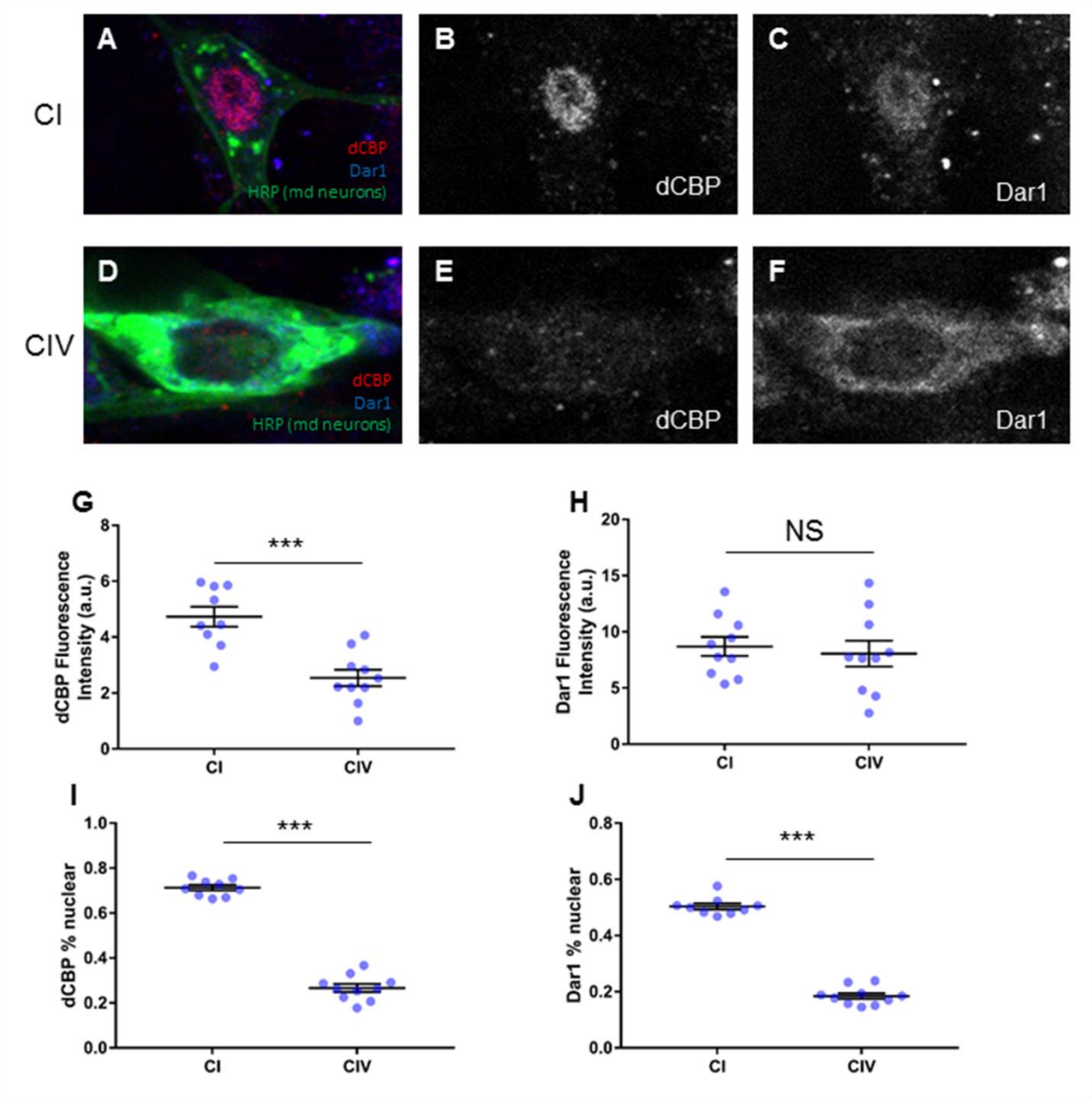

Figure 2.4 dCBP and Dar1 exhibit differential subcellular localization in md neuron subclasses.

(A-F) Representative images of wild-type dorsal md neurons showing dCBP (B, E) and Dar1 (C, F) protein localization in the morphologically simple CI md neurons (A-C) and the complex CIV md neurons (D-F). (G, H) Quantification of the total amounts of dCBP and Dar1 proteins present in CI and CIV neurons. (I, J) Quantification of the percentage of dCBP and Dar1 proteins localized to the nucleus in CI vs. CIV neurons. ***=$p<0.001$, NS=not significant. HRP labels all md sensory neurons.

2.2.3 dCBP regulates Dar1 subcellular localization and has Dar1-independent effects on dendritic morphology

We next asked whether dCBP could be involved in regulating the subcellular localization of Dar1. IHC analyses revealed that when *dCBP* is knocked down in CIV neurons, total Dar1 levels are not significantly changed relative to controls ($p=0.7006$) but the protein fails to maintain its normal cytoplasmic localization ($p<0.0001$) (**Fig. 2.5 A-E**), strongly supporting the hypothesis that dCBP is required to maintain the cytoplasmic localization of Dar1 in CIV neurons and that this change in subcellular Dar1 localization may be important in mediating the CIV morphological change. This interpretation is further supported by the observation that with Dar1 overexpression in CIV neurons, the Dar1 protein exhibits increased nuclear localization, consistent with what is observed with *dCBP* knockdown (**Fig. 2.5 B, C**). In fact, morphological comparison via Sholl analysis reveals a near phenocopy of dendritic defects between CIV-specific *dCBP* knockdown and CIV-specific Dar1 overexpression, given that both the maximum radius and the radius at which the maximum number of intersections occur for dCBP knockdown and Dar1 overexpression are significantly decreased from control neurons but do not differ from each other (**Fig. 2.5 F-H**) (see **Table S2** for specific p-values).

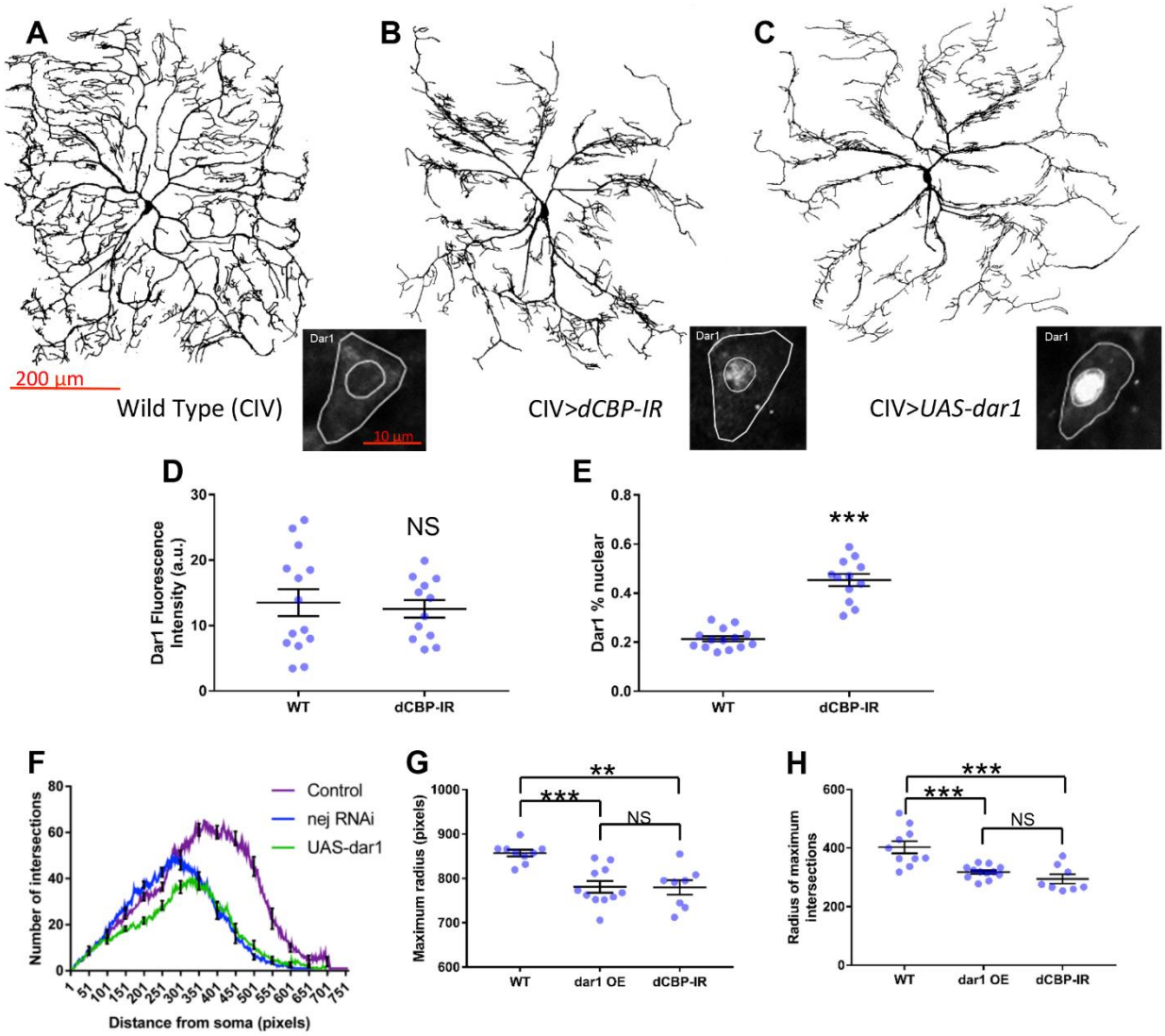

Figure 2.5 dCBP regulates Dar1 subcellular localization.

(A-C) Representative CIV images, with insets documenting effects of dCBP-IR knockdown or UAS-dar1 overexpression on Dar1 expression and subcellular localization. (D, E) Quantitative analyses of total Dar1 levels and percent of total Dar1 in the nucleus. (F-H) Quantitative Sholl analyses of dCBP RNAi vs. Dar1 overexpression. **=p<0.01; ***=p<0.001, NS=not significant.

We next asked whether Dar1 may have reciprocal regulatory effects on dCBP expression or subcellular localization. Dar1 overexpression experiments revealed a significant increase in the amount of dCBP present in the cell ($p<0.0001$), and both Dar1 and dCBP become highly nuclear (**Fig. 2.6 H, I, K, M)**. This suggests that nuclear Dar1 may be sequestering dCBP in the nucleus and that this effect may be contributing to a morphological change. In contrast, overexpression of dCBP, although it creates a drastically altered morphological phenotype (see

Fig. 2.3 C), does not change the level of expression (p=0.1028) or the subcellular localization (p=0.1998) of Dar1 (**Fig. 2.6 F, J, L**). This suggests that in addition to maintaining the cytoplasmic localization of Dar1 in CIV md neurons, dCBP regulates dendritic morphology via a Dar1-independent mechanism.

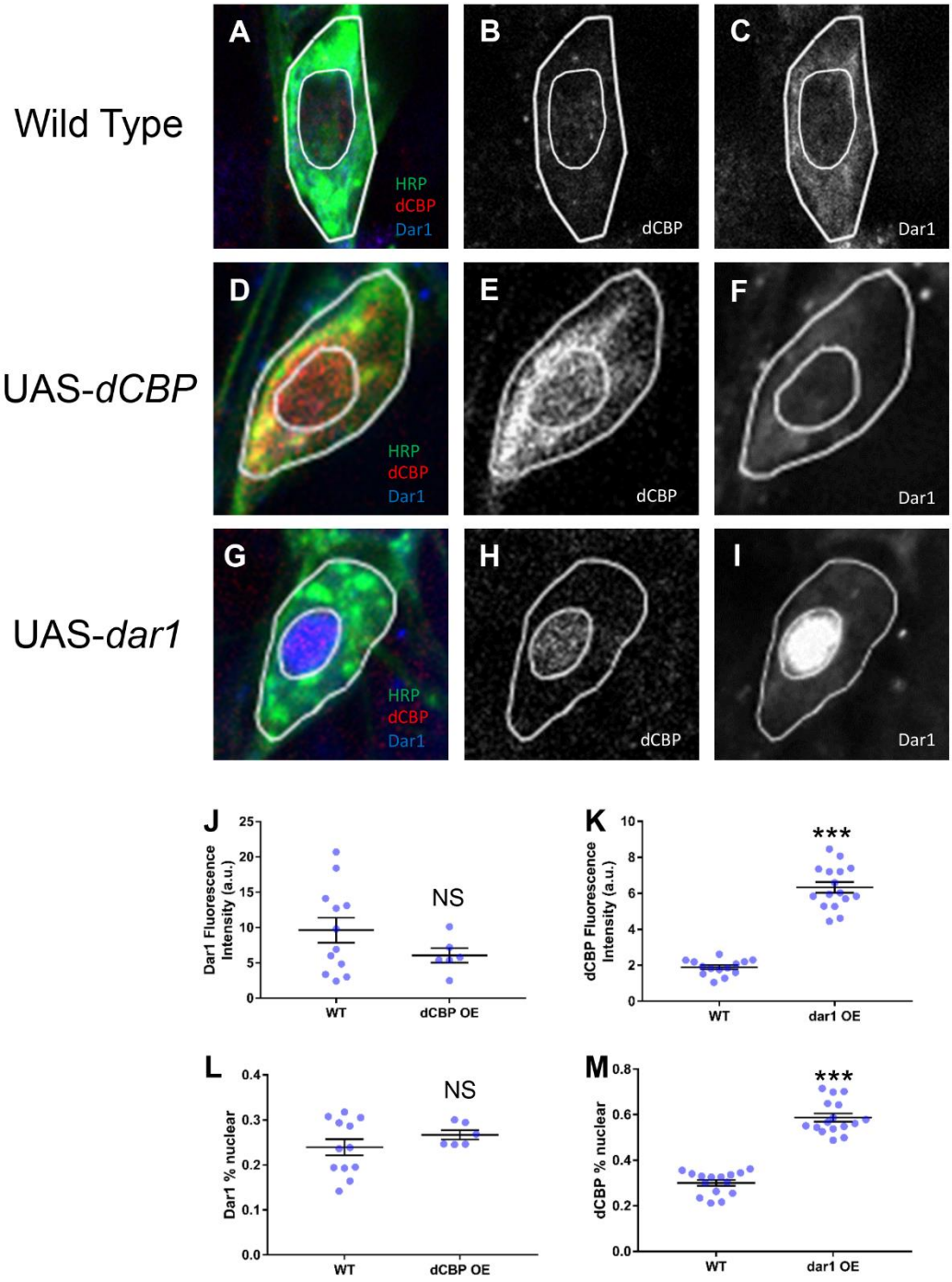

Figure 2.6 Dar1 overexpression promotes nuclear localization of both Dar1 and dCBP.

(A-I) IHC analysis of Dar1 and dCBP expression patterns in neurons overexpressing dCBP or Dar1. Representative images of WT (A-C), UAS-dCBP (D-F), and UAS-dar1 (G-I) Class IV md neurons triple labeled with HRP, anti-dCBP, and anti-Dar1. (J-M) Quantification of Dar1 and dCBP fluorescence intensities and percent of signal in the nucleus. ***=$p<0.001$; NS= not significant.

2.2.4 dCBP-mediated modulation of Dar1 localization is essential for proper dendrite morphogenesis

To characterize the potential molecular mechanisms by which dCBP and Dar1 may interact to direct cell type-specific dendritic morphogenesis and to further characterize the role of dCBP in this process, we conducted dCBP structure-function phenotypic analyses. CIV-driven expression of *dCBP* structure-function mutations (ΔdCBP) was used to explore the putative mechanistic requirements for dCBP protein domains in modulating CIV dendritic architecture (**Fig. 2.7 A**). The KIX, ΔBHQ, ΔHQ, ΔQ, and ΔNZK structure-function mutations are believed to exert their effects by competitive inhibition of native dCBP (Kumar et al. 2004), while the ΔH mutant has an inactivated histone acetyltransferase (HAT) domain.

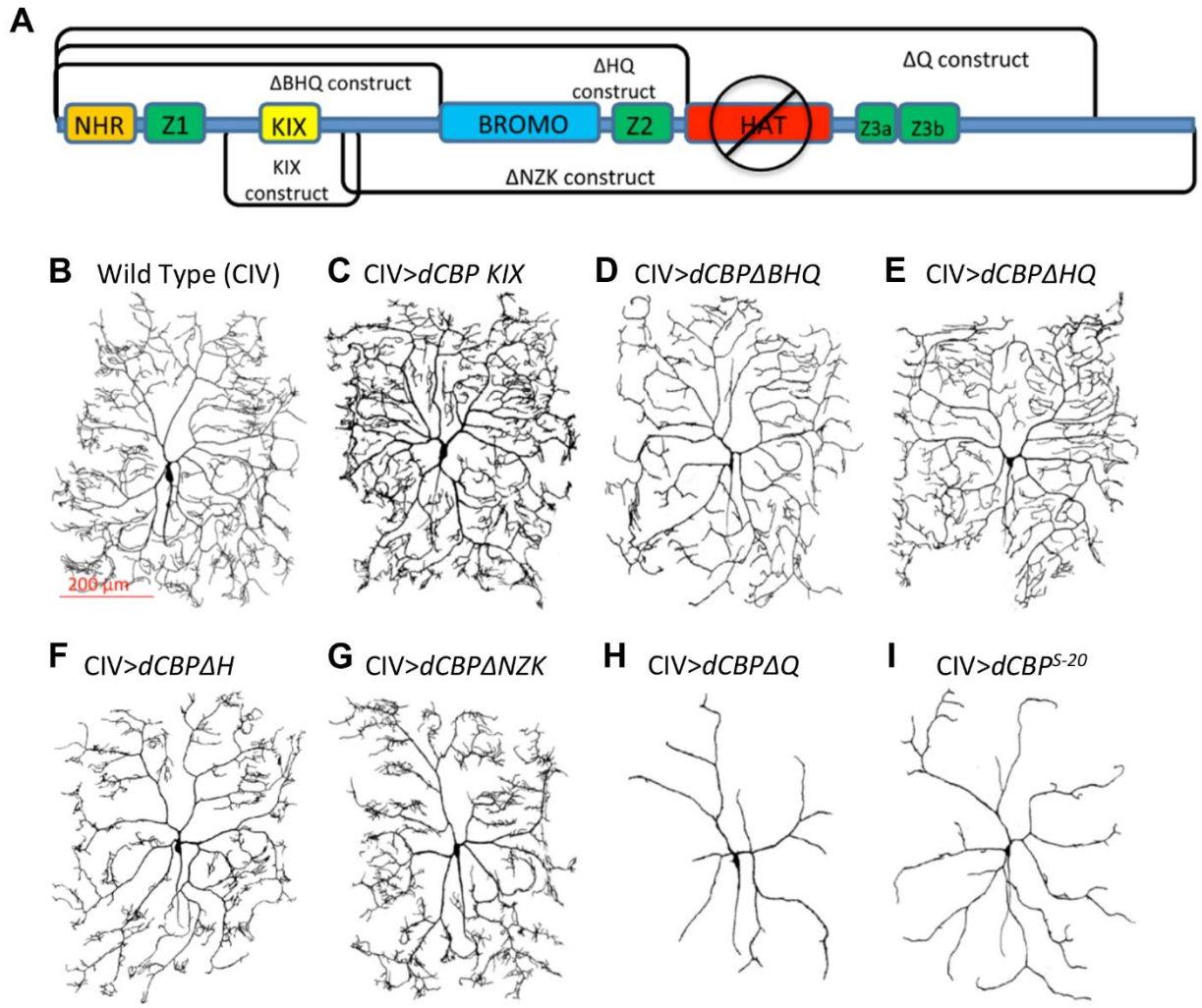

Figure 2.7 dCBP structure-function mutations.
(A) Schematic (adapted from Kumar et al. 2004) mapping the domains of the dCBP protein (relative positions and sizes) and the structure-function mutant transgenes used in our experiments. (B-I) Representative images of CIV neurons expressing the various dCBP structure-function mutant transgenes.

We paired phenotypic analyses (**Figs. 2.7, 2.8**) with IHC studies (**Fig. 2.9**) to investigate which domains of dCBP may mediate its interaction with Dar1. Mammalian CBP physically interacts with KLF5, the closest mammalian ortholog of Dar1, at the N-terminus of both proteins (Zhang and Teng 2003). Based on this, we predicted that the ΔBHQ, ΔHQ, and ΔQ constructs would interact normally with Dar1, while the ΔNZK and KIX constructs would be unable to interact with Dar1 due to N-terminal truncation. Our analyses revealed that expression of the

KIX domain alone had no significant effect on CIV dendritogenesis, suggesting that dCBP's regulatory control of CIV dendritic complexity is likely independent of its CREB-binding function (**Figs. 2.7 C, 2.8 A-E**). Moreover, KIX construct expression causes no change in the percentage of Dar1 present in the nucleus (**Fig. 2.9 A**). Expression of the ΔNZK construct causes no change in Dar1 nuclear localization (**Fig. 2.9 B**), but shows a reduction in dendritic field coverage (**Fig. 2.8 D)** and a branching pattern exhibiting short, clustered dendritic filopodia (**Fig. 2.7 G)**, similar in appearance to a CIII md neuron (note that the dCBP antibody used in Fig. 13 does not recognize the KIX or ΔNZK constructs, so the dCBP signal for both of these only accounts for native dCBP protein). In contrast, the ΔBHQ and ΔQ constructs both show a significant increase in both dCBP (ΔBHQ $p=0.0009$, ΔQ $p<0.0001$) and Dar1 (ΔBHQ $p=0.0008$, ΔQ $p<0.0001$) localization in the nucleus (**Fig. 2.9 C, E**), while ΔHQ shows a modest but significant increase in dCBP nuclear localization ($p=0.0408$) and an increase in Dar1 nuclear localization that approaches significance ($p=0.0652$) along with reductions of varying severity in higher order branching and field coverage (**Fig. 2.8 A-E**). We also found that expression of a *dCBP* transgene which has an inactivated HAT domain (ΔH) caused reduced dendritic growth and branching, suggesting that HAT domain function is required for normal CIV dendritogenesis (**Fig. 2.8 A-E**). In the case of the ΔQ construct and expression of the *UAS*-inducible $dCBP^{S-20}$ insertion, the dendritic arbor is severely reduced down to major and intermediate (1^{st} through 4^{th} order) branches only (**Figs. 2.7 H, I, 2.8 E**), which is consistent with the effects observed with full-length dCBP overexpression (**Fig. 2.2 C**).

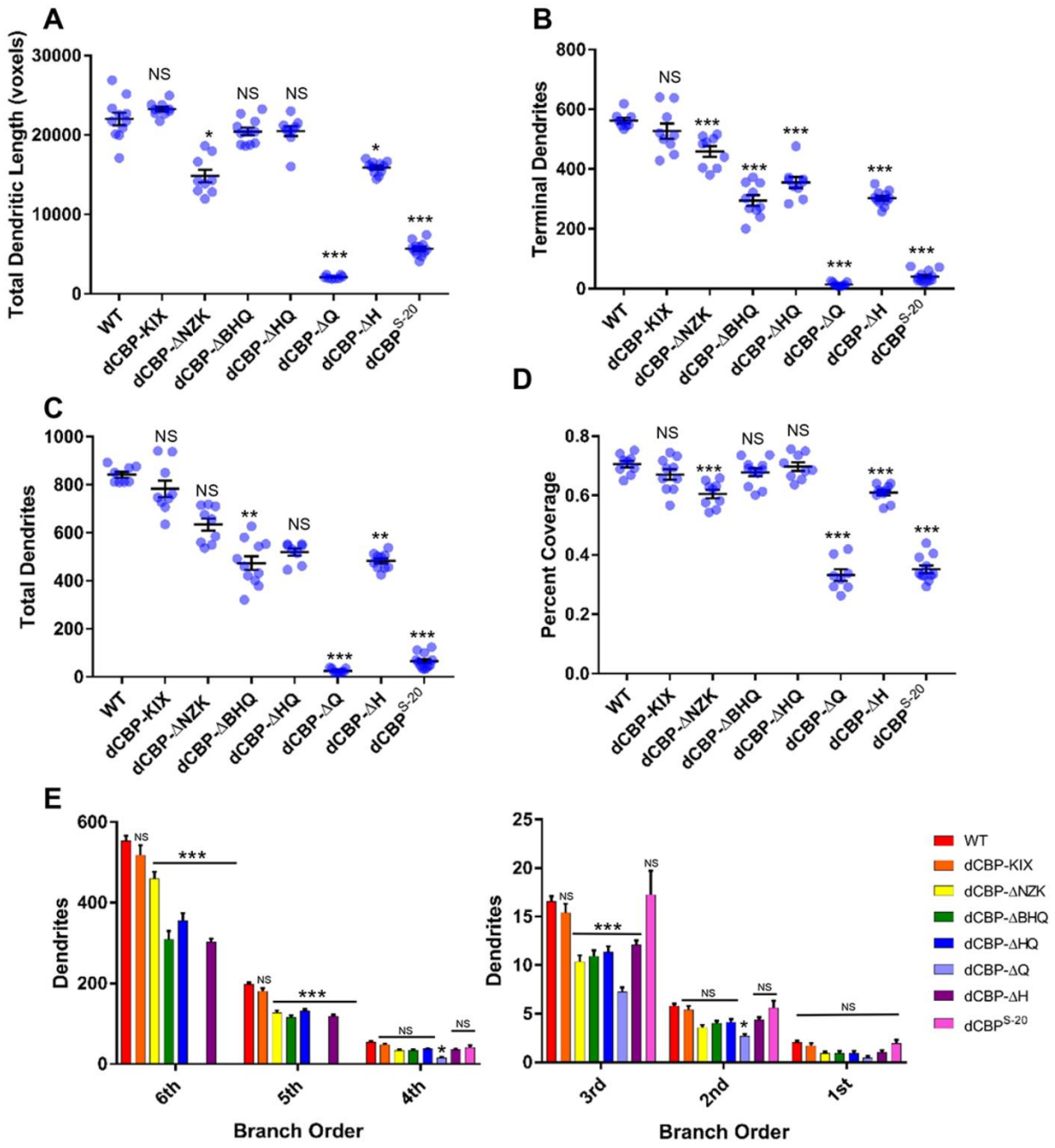

Figure 2.8 Dendritic morphology of dCBP structure-function mutant neurons.

(A-E) Morphological quantification of CIV neurons expressing the various dCBP structure-function mutant transgenes. dCBP-ΔQ and dCBP^{S-20} do not have branches beyond 4th order. *=p<0.05; ***=p<0.01; ***=p<0.001; NS=not significant.

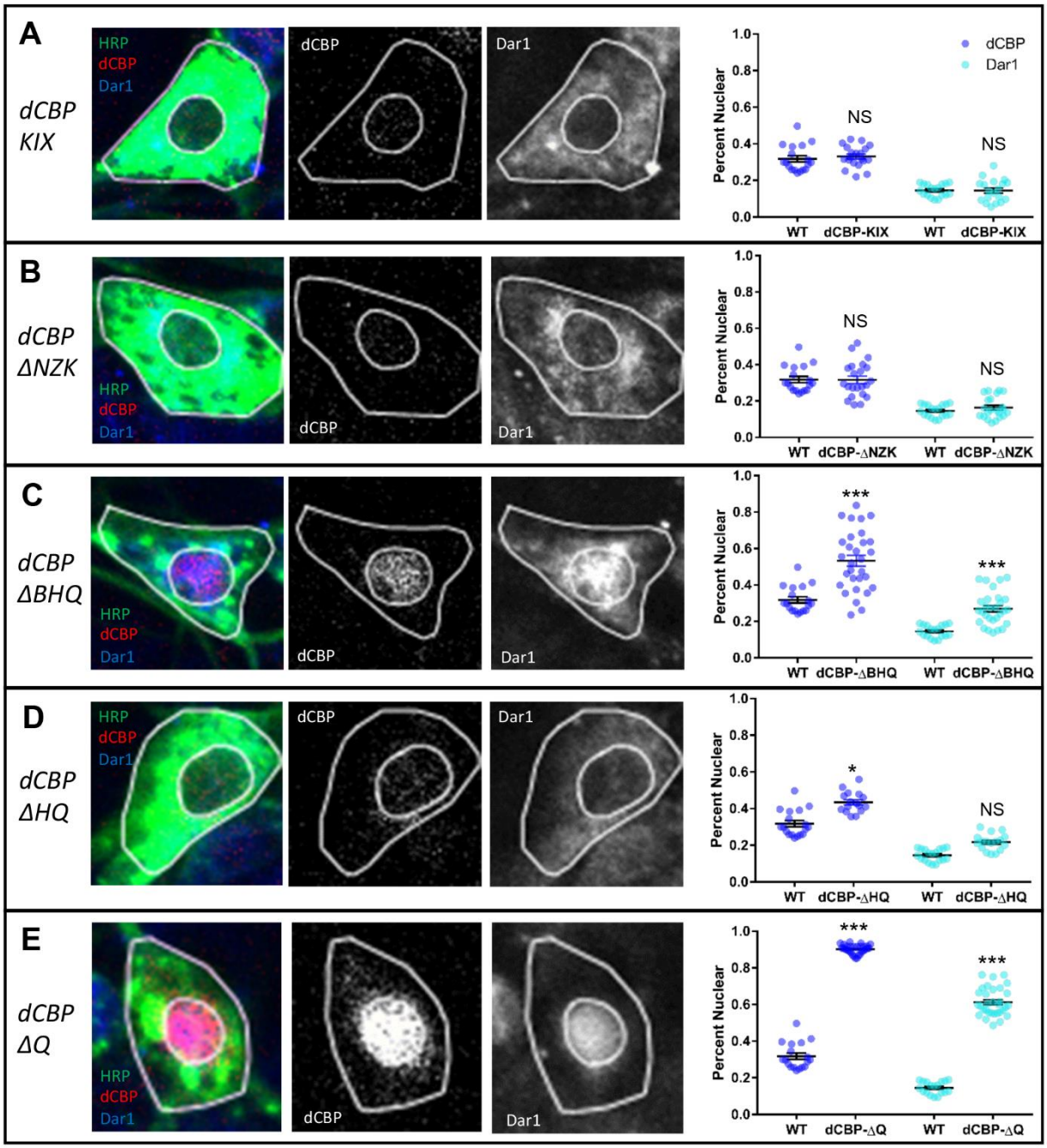

Figure 2.9 dCBP-mediated modulation of Dar1 localization is essential for proper dendrite morphogenesis.

(A-E) The first three columns show representative IHC images of dorsal CIV md neurons stained with HRP, anti-dCBP, and anti-Dar1 (as labeled). The last column shows IHC analysis of percent localization of Dar1 and dCBP in CIV md neurons for each of the domain deletions. *=p<0.05; ***=p<0.001; NS=not significant.

Collectively, these data suggest specific roles for different dCBP protein domains in Dar1 and dCBP localization and reveal the contribution of dCBP domains to establishing proper dendritic branching and field coverage. Furthermore, these analyses are indicative of a role for dCBP in the specification of dendritic morphology that is independent of its influence on the subcellular localization of Dar1.

2.3 Materials and Methods

2.3.1 Drosophila genetics

Drosophila stocks were maintained at 25°C on standard molasses-cornmeal agar. The following strains were obtained from Bloomington *Drosophila* Stock Center: UAS-RNAi lines directed against dCBP (27724, 37489), *UAS-dCBP*, *UAS-dCBP*$^{S-20}$ and *UAS-dCBPΔH*. Additional strains from other sources included the class I md reporter strain *GAL4*^{221}*,UAS-mCD8::GFP*; the class IV md neuron reporter strain *GAL4*^{477}*,UAS-mCD8::GFP; ppk1.9-GAL4,UAS-mCD8::GFP*; *dar1*^{D6} (gift from J. Kassis, NIH; Ye et al. 2011); and *dar1*^{f01014} (Exelixis collection, Harvard). To investigate the putative functional roles of dCBP domains, the following structure-function transgenes were used: *UAS-dCBPΔNZK; UAS-dCBPΔQ; UAS-CBPΔHQ; UAS-dCBPΔBHQ;* and *UAS-dCBP-KIX* (Kumar et al. 2004). The *UAS-dar1* transgene used in these analyses was generated by cloning the full length *dar1* cDNA into a FLAG-tagged *pUAST* vector. Transformant lines were generated by BestGene, Inc. Detailed genotypes for each figure are reported in **Table S1**.

2.3.2 Immunofluorescent Labeling

Dissection and immunofluorescent labeling of third instar larval filets was performed as previously described (Sulkowski et al. 2011). Primary antibodies used in this study include: guinea pig anti-dCBP (gift from M. Mannervik used at 1:200); rabbit anti-Dar1 (gift from J. Kassis, NIH used at 1:200); rabbit anti-CBP (LSBio, used at 1:100); and Dylight AffiniPure Goat anti-horseradish peroxidase (HRP) 488 conjugated (1:200). Secondary antibodies used include: donkey anti-guinea pig (1:400) (Jackson Immunoresearch) and donkey anti-rabbit (1:200) (Life Technologies). Filets were imaged on either a Nikon C1 Plus confocal microscope or a Zeiss LSM780 confocal microscope. Fluorescence intensities were quantified using the Measure function in Photoshop (Adobe) and were normalized to area to control for differences in md neuron subclass cell body size. Identical confocal settings for laser intensity and other image capture parameters were applied for comparisons of control vs. experimental samples.

2.3.3 Live Imaging Confocal Microscopy, Neuronal Reconstruction, and Morphometric Data Analyses

Live neuronal imaging was performed as previously described (Iyer S et al. 2013, Iyer E et al. 2013). We focused on the dorsal cluster of md neurons including C-I ddaE neurons and C-IV ddaC neurons as morphological representatives of these md neuron subclasses. Dendritic morphology was quantified as previously described (Iyer E et al. 2013). Briefly, maximum intensity projections of confocal Z-stacks were exported as a jpeg or TIFF. Once exported, images were manually curated to eliminate non-specific auto-fluorescent spots (such as the larval

denticle belts) using a custom designed program, *Flyboys* (freely available upon request). For total dendritic length measurements, images were processed and skeletonized in ImageJ (Iyer E et al. 2013, Schneider et al. 2012). Quantitative neuromorphometric information was extracted and compiled using custom Python algorithms. The custom Python scripts were used to compile the output data from the Analyze Skeleton ImageJ plugin and the compiled output data was imported into Excel (Microsoft). For total dendritic branches and number of terminal branches, images were reconstructed using NeuronStudio (Wearne et al. 2005). Branch number and order were then extracted using the centripetal branch labeling function and output data was compiled in Excel.

2.3.4 Statistical Analysis and Data Availability

Statistical analyses of neuromorphometric and IHC data and data plotting were performed using GraphPad Prism 7. Error bars reported in the study represent SEM. Statistical analyses were performed using either two-tailed unpaired t-test with Welch's correction or one-way ANOVA using Dunnett's multiple comparisons test when data sets were normally distributed as determined by the Shapiro-Wilk normality test. When data was not normally distributed, appropriate non-parametric tests were used (see **Table S2** for specific tests used in each case). Significance scores indicated on graphs are (*=$p \leq 0.05$, **=$p \leq 0.01$, ***=$p \leq 0.001$). Detailed information on statistical analyses for each figure is reported in **Table S2**.

3 DCBP UTILIZES TRANSCRIPTIONAL REPRESSION TO REGULATE CELL TYPE-SPECIFIC DENDRITOGENESIS VIA CYTOSKELETAL REGULATORS

3.1 Scientific Premise

The studies described in Chapter 2 establish a functional requirement for dCBP in directing cell type-specific dendritic arborization by regulating the subcellular localization of the transcription factor Dar1, but also suggested that dCBP plays a role in dendritic morphogenesis that is independent of its interaction with Dar1. Phenotypic analyses revealed that knockdown of dCBP (*dCBP-IR*) (**Fig. 2.5 B**) and expression of the **Δ**NZK deletion transgene (**Fig. 2.7 G**) produce similar defects in CIV neurons, altering the dendritic arborization branching patterning (**Fig. 2.3 D-F, H; Fig. 2.8 A-E)**, however *dCBP-IR* expression leads to a shift in Dar1 expression from largely cytoplasmic localization to nuclear expression relative to control (**Fig. 2.5 A, B**), whereas expression of **Δ**NZK does not shift Dar1 to a nuclear location and does not alter Dar1 levels (**Fig. 2.9 B**). Thus, the dendritic defects observed with **Δ**NZK deletion suggest a role for other interactors in addition to Dar1 in dCBP-mediated dendritogenesis. To that end, we sought to identify and characterize Dar1-independent mechanisms by which dCBP regulates cell-type specific dendritic development.

To characterize dCBP-mediated transcriptional regulation in CIV neurons, we performed RNA sequencing (RNAseq) analyses of isolated CIV neurons expressing dCBP variants. Specifically, we selected the two *dCBP* deletion constructs that had profound effects on CIV dendritic arborization: the ΔQ (mimicking *dCBP* gain-of-function effects) and the ΔNZK (mimicking *dCBP-IR* loss-of-function effects). The Bromo, Z2, HAT, and Z3 functional domains are overexpressed in the cases of both the ΔQ and ΔNZK constructs (black box in **Fig. 3.1**),

while the NHR, Z1, and KIX domains are overexpressed in the case of the ΔQ construct but are not present in the ΔNZK construct (green box in **Fig. 3.1**). Therefore, differential expression of genes between WT control CIV neurons and ΔQ CIV neurons or between WT and ΔNZK CIV neurons could be due to the overexpression of any of the domains shared by the ΔQ and ΔNZK constructs. However, the intersection of the sets of genes differentially expressed between WT and the ΔNZK construct and the genes differentially expressed between the ΔNZK and ΔQ constructs represent genes that have failed to be regulated due to the loss of the NHR, Z1, and/or KIX domains in the ΔNZK construct. These genes are therefore the most likely to be implicated in the dendritic abnormalities associated with the ΔNZK phenotype.

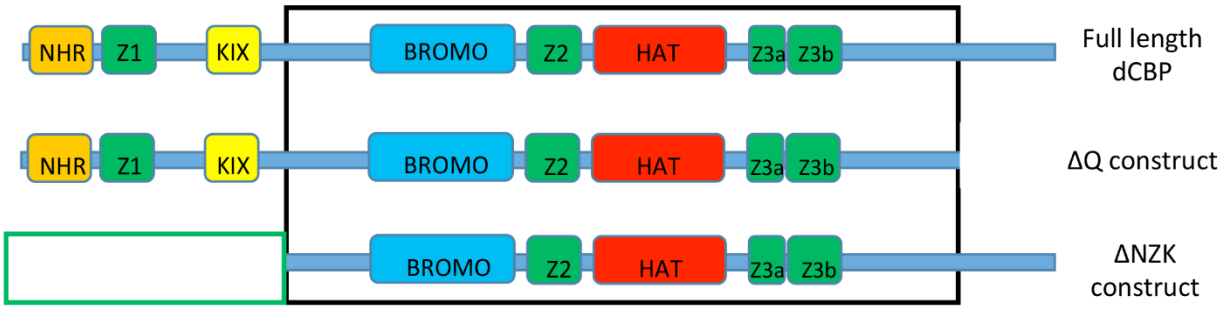

Figure 3.1 dCBP schematic.
Wild type, ΔNZK, and ΔQ dCBP with domains shown in relative positions and sizes.

Cytoskeletal effectors are common targets of the transcriptional regulation that contributes to class-specific dendritogenesis (Jinushi-Nakao et al. 2007; Iyer et al. 2012; Ye et al. 2011; Nagel et al. 2012; Das et al. 2017) as cytoskeletal organization and dynamics play a pivotal role in driving neuronal cell shape. We therefore chose to examine the potential effects that the ΔNZK construct may have on F-actin and microtubule (MT) cytoarchitecture in CIV md neurons. When compared to the ΔQ construct, which has strong effects on both dendritic morphology and Dar1 localization (**Fig. 2.7 H; Fig. 2.9 E**), the ΔNZK construct appears similar

in its ability to enhance F-actin levels in CIV neurons but differs in that it also appears to enhance MT levels, whereas the ΔQ construct appears to cause disruptions in MT organization (**Fig. 3.2 insets**). Specifically, we observed that expression of the ΔNZK deletion construct leads to a qualitative increase in the intensities of both the F-actin and MT cytoskeletal levels, relative to controls. In the case of the MT signal, the increased levels in ΔNZK may indicate a more stabilized or perhaps bundled MT architecture which can impact dendritic growth and branching, as these processes are reliant on dynamic MT properties. In the case of the ΔQ deletion construct, the MT signal is notably disrupted (see arrow in **Fig. 3.2 C**, MT inset), whereas the F-actin signal is increased in intensity, relative to control. This suggests that perhaps one major function of dCBP may be to promote MT dynamics and/or MT-mediated processes that contribute to normal dendritic growth and branching. Based upon these preliminary qualitative phenotypic assessments and our differential gene expression analyses, we chose to further investigate the putative transcriptional role of dCBP in directing dendritic morphogenesis and cytoskeletal architecture.

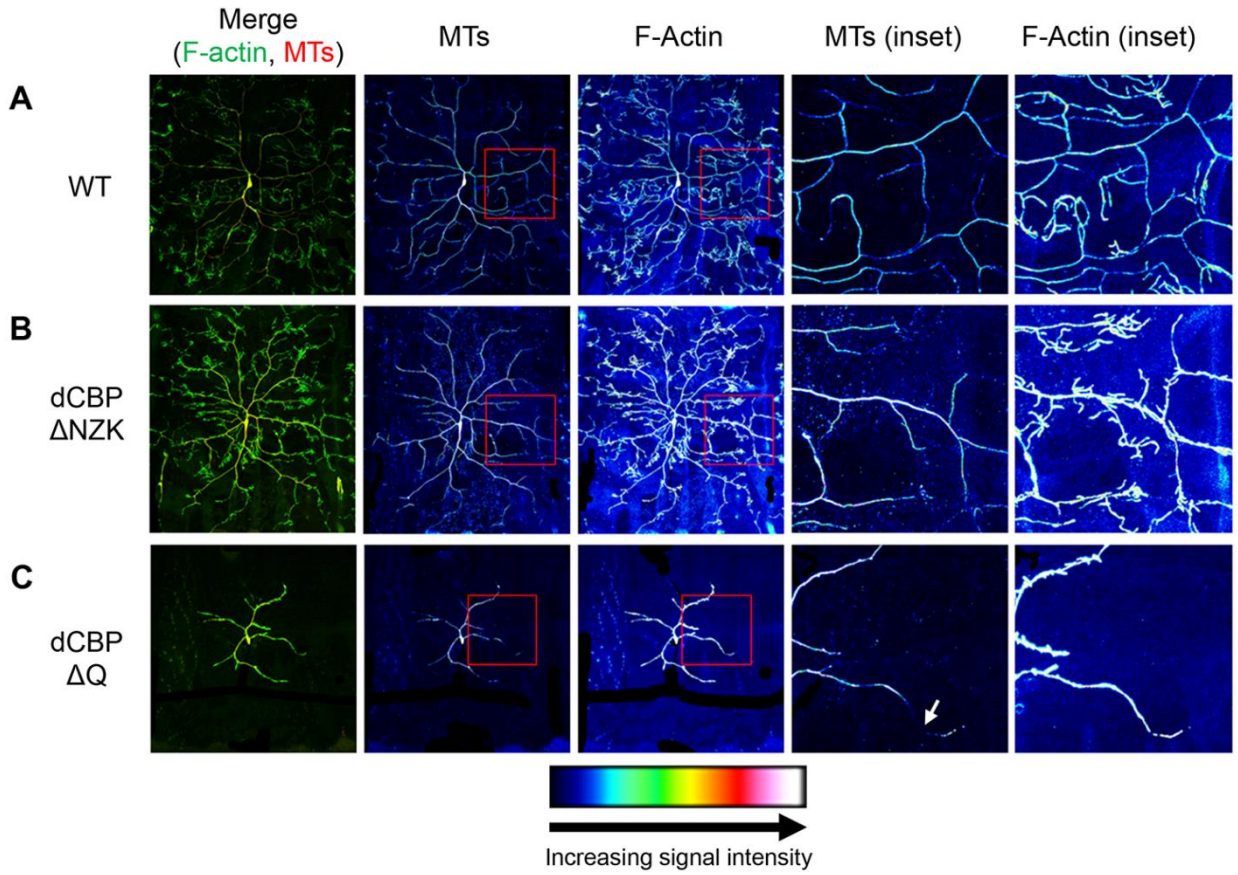

Figure 3.2 dCBP deletion constructs differentially affect cytoskeletal components.
(A-C) Wild type, ΔNZK, and ΔQ CIV md neurons expressing GMA, a GFP-tagged actin binding protein and mCherry-tagged Jupiter, a microtubule binding protein. The second through fifth columns show the intensity of the separated signals according to the key below the figure.

To determine whether differentially expressed genes of interest were involved in dCBP-mediated regulation of dendritic arborization and/or cytoskeletal dynamics, we utilized a phenotypic suppression approach (**Fig. 3.3**), focusing on the genes that exhibited increased expression in the ΔNZK background. In this approach, *UAS*-driven RNAi knockdown of a gene of interest is combined with expression of the ΔNZK construct in CIV md neurons. In the case of genes that are involved in dCBP-mediated regulation of dendritic arborization and/or cytoskeletal dynamics, we expect to see a suppression of the ΔNZK phenotype resulting in a morphological rescue back towards normal CIV morphology. In the case of genes that are not

involved in dCBP-mediated regulation of dendritic arborization and/or cytoskeletal dynamics, we expect to see the ΔNZK phenotype persist.

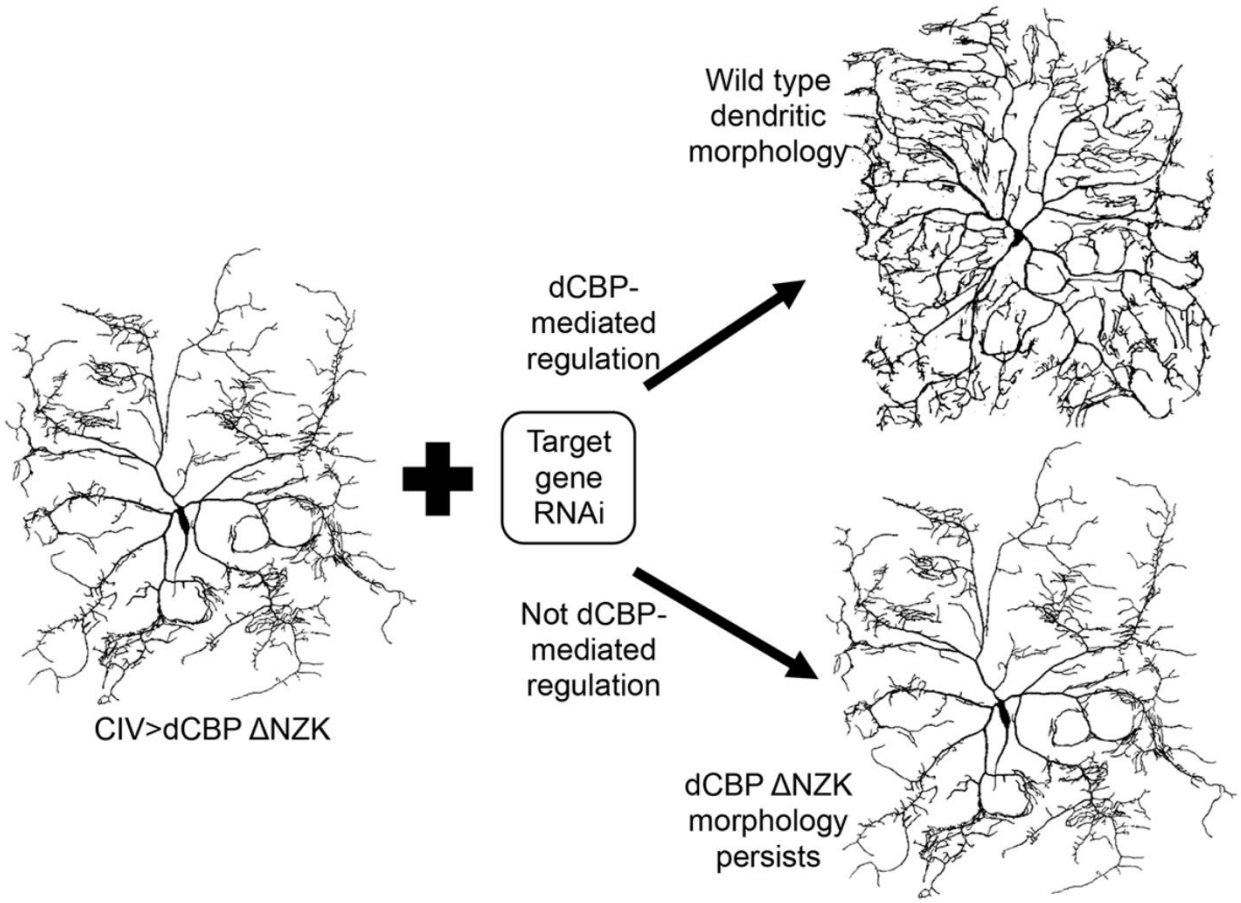

Figure 3.3 Graphic representation of phenotypic suppression screen approach.

3.2 Results

3.2.1 dCBP ΔNZK expression predominately results in release of transcriptional repression

To characterize dCBP-mediated transcriptional regulatory effects that may underlie the phenotypic defects observed with the ΔNZK and ΔQ structure-function variants, we performed large-scale magnetic bead cell isolations for the ΔNZK and ΔQ constructs and for WT CIV md neurons, then extracted RNA from these cells for cell type-specific RNAseq analyses. We then subjected RNAseq results from WT, ΔQ and ΔNZK CIV samples to bioinformatic differential expression analyses according to the workflow diagram in **Fig. 3.4 A**. We then selected the genes most likely to be implicated in the ΔNZK phenotype by determining the intersection of the sets of genes differentially expressed between WT and the ΔNZK construct and the genes differentially expressed between the ΔNZK and ΔQ constructs. This analysis resulted in a list of ~600 genes (**Fig. 3.4 B, C**). Intriguingly, most of these differentially expressed genes demonstrate increased expression in the presence of the ΔNZK deletion construct. These findings imply that a major function of dCBP-mediated regulation of dendritic morphogenesis may involve repression of target gene transcription in CIV neurons (**Fig. 3.4 B**). We next subjected this list of differentially expressed genes to ontological clustering using DAVID. Gene clusters of particular interest that were enriched in the analysis included phosphorylation, ubiquitination, microtubule-based processes, protein modification processes, cytoskeletal organization, and cell morphogenesis, among others (**Fig. 3.4 D**). We selected these clusters due to their putative involvement in cytoskeletal processes that appear to be disrupted in the ΔNZK and ΔQ deletion constructs, as shown in **Fig. 3.2**. A full list of the 23 genes selected for further phenotypic analyses is presented in the **Appendix**.

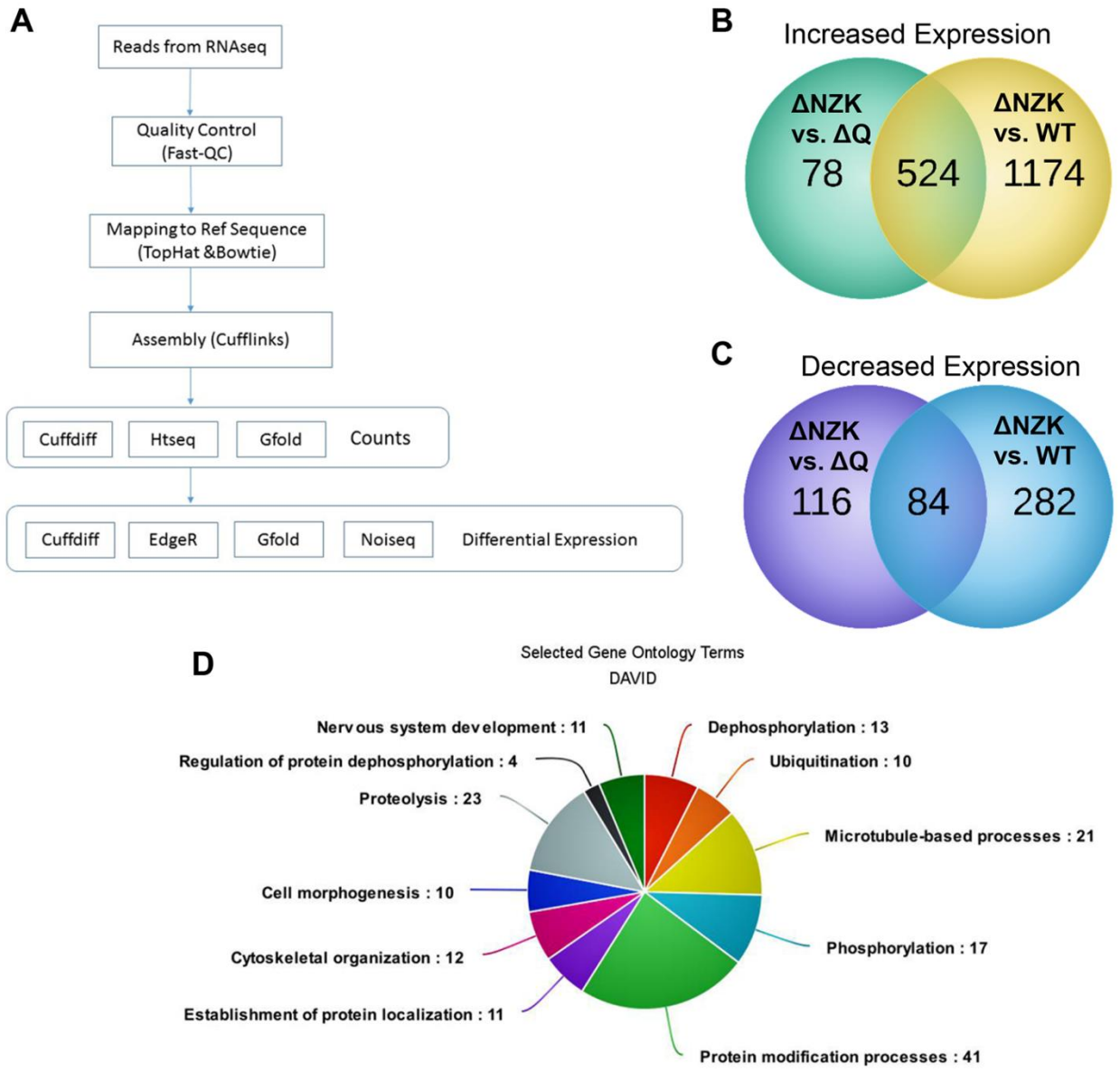

Figure 3.5 RNAseq workflow, results, and gene ontological clustering.

(A) Diagram of the workflow for analysis of RNAseq read counts. (B-C) Numbers of genes exhibiting differential expression in relevant comparisons. (D) Gene ontology clusters selected for further analysis, showing number of differentially expressed genes in each cluster (some genes appear in more than one cluster).

3.2.2 Seven genes of interest exhibit partial rescue of the dCBP ΔNZK phenotype

The ΔNZK phenotype exhibits multiple apparent morphological defects, including localized over-proliferation of terminal branches at the expense of intermediate branches, loss of field coverage, and a decrease in total dendritic length (**Figs. 3.6-3.9**). For the purposes of the phenotypic suppression screen, at least two independent gene-specific RNAi (IR) lines for each gene of interest were tested and lines that exhibited qualitative rescue of at least one aspect of the morphological defects observed in the ΔNZK phenotype were selected for detailed quantitative analysis. Of the 23 genes selected for the phenotypic suppression screen, seven exhibited notable rescue of at least one ΔNZK morphological defect. These genes were *Actin-related protein 53D* (*Arp53D*) (**Fig. 3.5 C**), *CG10177* (**Fig. 3.5 D**), *CG32238* (**Fig. 3.5 E**), *α-actinin 3 (Actn3)* (**Fig. 3.5 F**), *CG12620* (**Fig. 3.5 G**), *CG31391* (**Fig. 3.5 H**), and *CG16716* (**Fig. 3.5 I**).

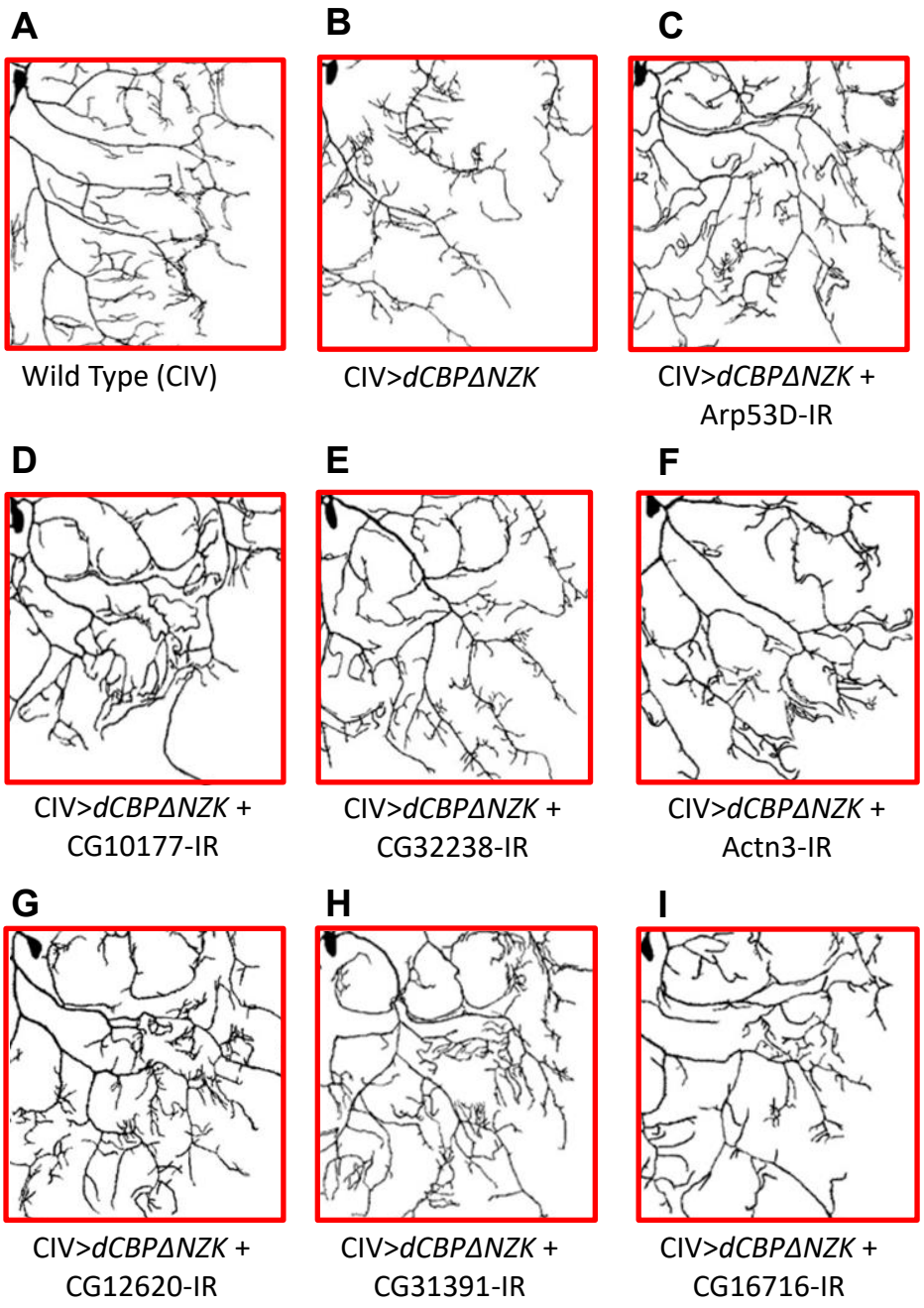

Figure 3.6 Seven genes of interest exhibit partial rescue of the ΔNZK phenotype.

Representative images of ΔNZK + gene-specific RNAi CIV neurons exhibiting morphological rescue of at least one aspect of ΔNZK morphological deficits.

3.2.3 Actn3 and CG31391 knockdowns rescue ΔNZK-induced deficits in major and intermediate order branching

One of the morphological defects evident in ΔNZK CIV md neurons is a change in branch order distribution to favor clusters of terminal branches with fewer intermediate branches over the more regular distribution apparent in WT CIV md neurons (Fig. 3.6 C). Quantitatively, this manifests as a significant decrease from WT in Strahler Order 3 branches ($p=0.0022$) (Fig. 3.6 B) as well as branches of Strahler Order 4 and greater ($p=0.0163$) (Fig. 3.6 A). The Strahler Order of branches is counted from the terminal branches towards the cell body, thus "Strahler Order 4+" designates the group of major branches most directly connected to the cell body, while "Strahler Order 3" designates the intermediate branches one step removed from the major branches. The ΔNZK-induced deficit in major branches is rescued only by knockdown of CG31391 ($p=0.0185$) (Fig. 3.6 A, E), which encodes an ortholog of a protein-phosphatase 1 regulatory subunit. The deficit in intermediate branching, however, is rescued by knockdown of CG31391 ($p=0.0193$) as well as by knockdown of Actn3 ($p=0.0017$) (Fig. 3.6 B, D, E). *Actn3* encodes a putative actin-binding protein that contains a calponin homology domain, however its function is not well understood.

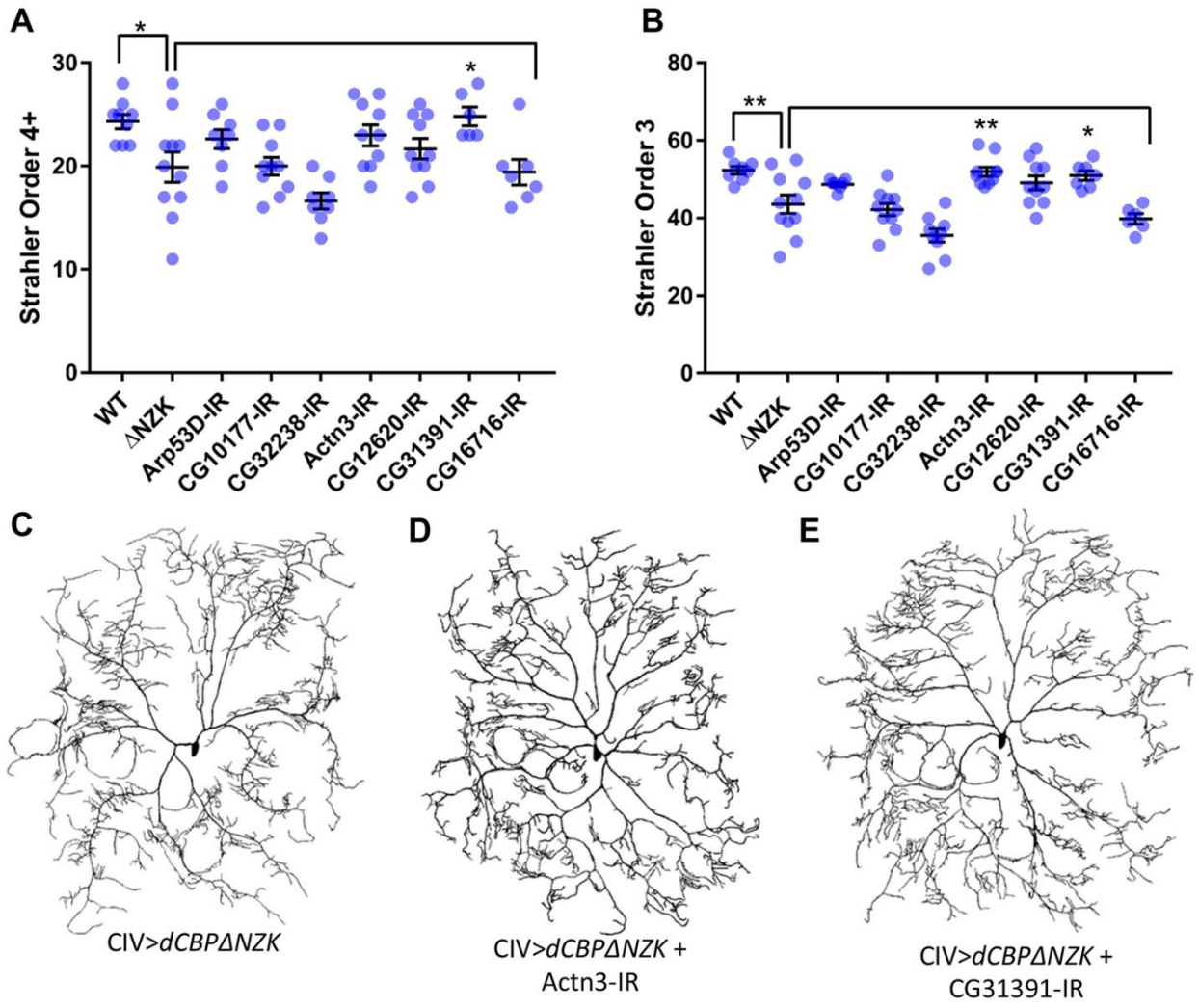

Figure 3.7 Actn3 and CG31391 knockdowns rescue ΔNZK-induced deficits in major and intermediate order branching.

(A) Quantification of dendrites of Strahler Order 4 or greater, which denotes major dendrites most proximal to the cell body. (B) Quantification of dendrites of Strahler Order 3, which denotes intermediate order dendrites. (C-E) Representative images of third instar larval CIV md neurons for dCBPΔNZK (C); dCBPΔNZK + Actn3-IR (D) and dCBPΔNZK + CG31391-IR (E).

3.2.4 Actn3, CG31391, CG16716, and CG12620 knockdowns rescue ΔNZK-induced deficits in spatial distribution of dendrites

Another apparent morphological defect induced by expression of the ΔNZK construct is a shift in the spatial distribution of dendrites. Specifically, the previously mentioned clusters of

terminal branches appear mainly in an area about halfway between the cell body and the maximum radius of the dendrites, leaving more "stripped" appearing branches both proximal and extremely distal to the cell body (**Fig. 3.7 C**). These stripped branches also tend to extend further from the cell body than major branches do in WT CIV neurons. Quantitatively, this results in a significantly increased maximum dendritic radius (p=0.0001) (**Fig. 3.7 A**) in ΔNZK CIV neurons along with a significant decrease in the radius at which the maximum number of intersections occur (p=0.0001) (**Fig. 3.7 B**) according to Sholl analysis. The increased maximum radius is rescued by knockdowns of Actn3 (p=0.0060), CG31391 (p=0.0026), and CG16716 (p=0.0114) (**Fig. 3.7 A, D-F**) and knockdown of CG10177 approaches significance (p=0.0598), while the decrease in the radius at which the maximum number of intersections occurs is rescued by knockdown of CG12620 (p=0.0250) (**Fig. 3.7 B, G**), with knockdowns of Arp53D (p=0.0889) and CG16716 (p=0.0742) approaching significance. CG10177 encodes a MT-associated protein with doublecortin-like kinase activity which is thought to have a role in Golgi organization (Zacharogianni et al. 2011), among other potential roles. CG16716 encodes an ortholog of tubulin tyrosine ligase-like 6A, a tubulin polyglutamylase, and CG12620 encodes a protein ortholog of protein-phosphatase 1 regulatory subunit 2 (*H. sapiens* PPP1R2), which has been investigated as potentially influencing the development of non-insulin dependent diabetes in some populations (Permana and Mott 1997).

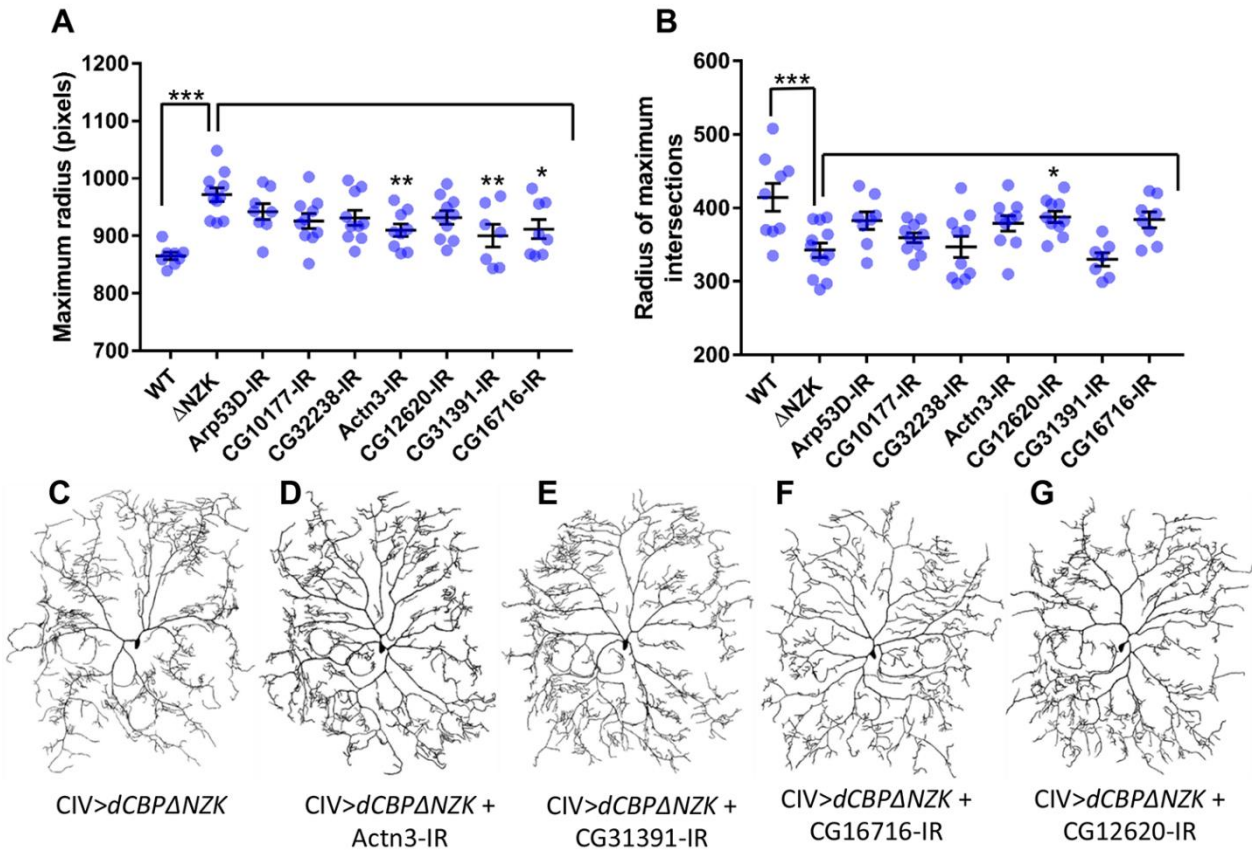

Figure 3.8 Actn3, CG31391, CG16716 and CG12620 knockdowns rescue ΔNZK-induced deficits in spatial distribution of dendrites.

(A) Quantification of Sholl analysis of the neuronal maximum radius. (B) Quantification of Sholl analysis of the radius at which the maximum number of intersections occur. (C-G) Representative images of third instar larval CIV md neurons for dCBPΔNZK (C); dCBPΔNZK + Actn3-IR (D); dCBPΔNZK + CG31391-IR (E); dCBPΔNZK + CG16716-IR (F); and dCBPΔNZK + CG12620-IR (G).

3.2.5 Actn3 knockdown rescues ΔNZK-induced deficits in total dendritic length

Expression of the ΔNZK construct also results in a significant decrease in the total dendritic length from WT CIV neurons (p=0.0005) (**Fig. 3.8 A, C**). This decrease occurs in spite of there being no change in the total number of dendrites (p=0.7573) (**Fig. 3.8 B**), indicating that the dendrites that are present are generally reduced in length. Moreover, this is consistent with the loss of major and intermediate order branches shown in Fig. 19. This decrease in total dendritic length is rescued by knockdown of Actn3 (p=0.0392), and knockdown of Arp53D

approaches significance (p=0.0553) (**Fig. 3.8 A, D**). *Arp53D* encodes an actin-related protein whose exact function is poorly understood.

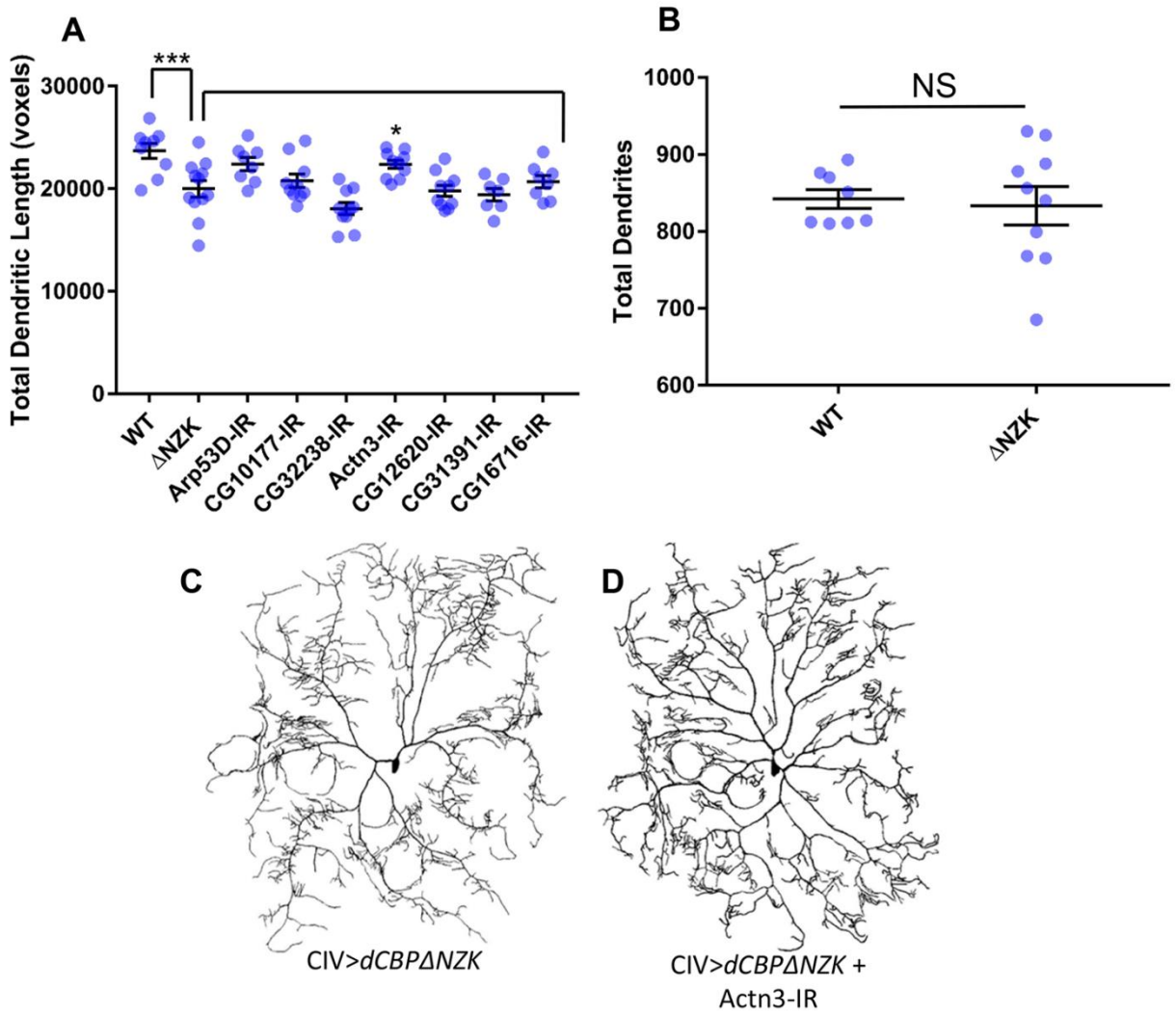

Figure 3.9 Actn3 knockdown rescues ΔNZK-induced deficits in total dendritic length.

(A) Quantification of total dendritic length (voxels). (B) Total number of dendrites in WT and ΔNZK neurons. (C, D) Representative images of third instar larval CIV md neurons for dCBPΔNZK (C) and dCBPΔNZK + Actn3-IR (D).

3.2.6 Arp53D, Actn3, and CG16716 knockdowns rescue ΔNZK-induced deficits in dendritic field coverage

Finally, expression of the ΔNZK construct results in deficits in dendritic field coverage. This parameter was measured using a Fiji macro (Sears and Broihier 2016) that populates a described area with squares and quantifies the number of squares that contain a signal (see **Fig. 3.9 A-E** for examples). The space-filling properties of WT CIV md neurons result in mainly positive (containing dendrite) squares within the space bounded by the dendritic arbor (**Fig. 3.9 A**) and this number is significantly decreased (p=0.0001) in the ΔNZK-expressing CIV neurons (**Fig. 3.9 B, F**). This decrease in coverage is rescued by knockdowns of Actn3 (p=0.0001) (**Fig. 3.9 C, F**), Arp53D (p=0.0005) (**Fig. 3.9 D, F**), and CG16716 (p=0.0246) (**Fig 3.9 E, F**). **Fig. 3.10** shows a summary of all of these results.

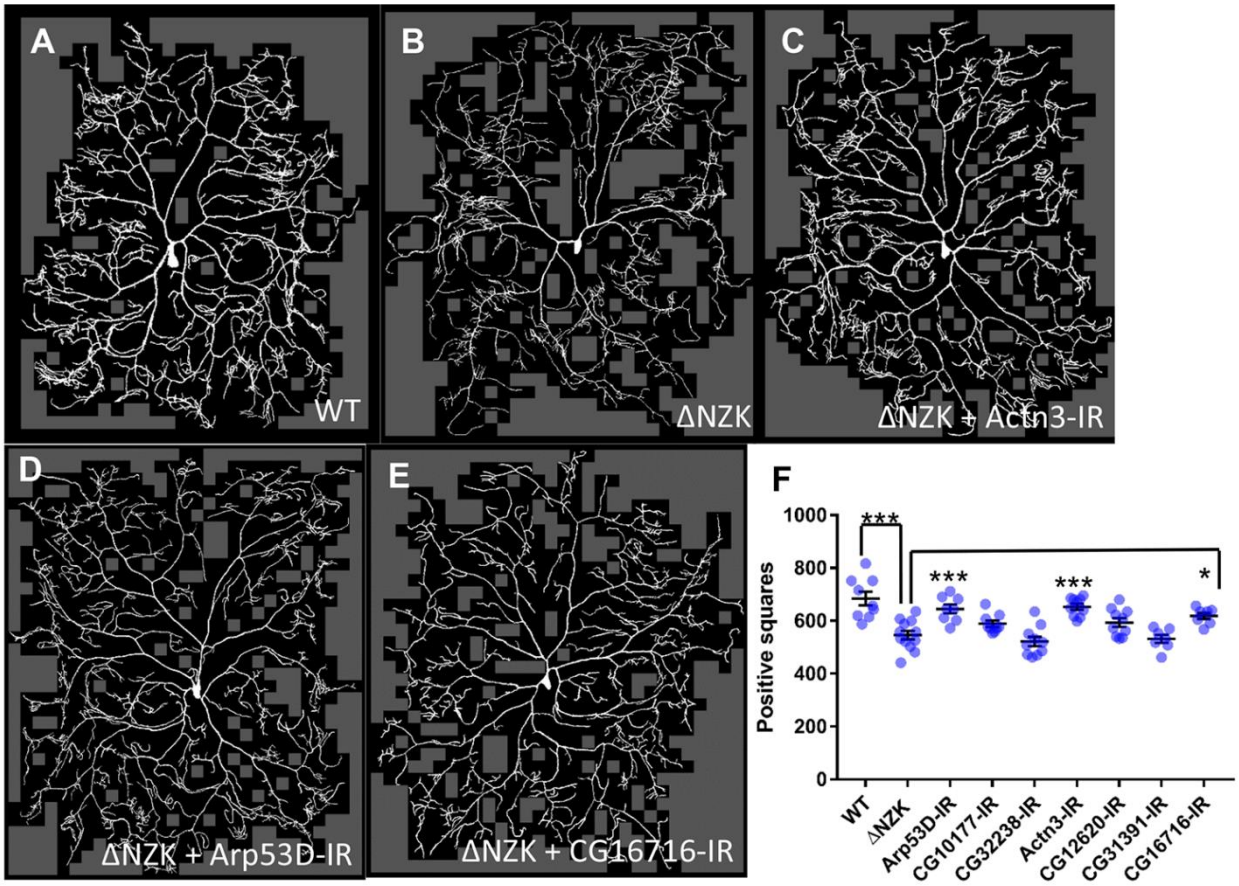

Figure 3.10 Arp53D, Actn3, and CG16716 knockdowns rescue ΔNZK-induced deficits in dendritic field coverage.

(A-E) Representative images of neurons processed using the Internal Field Coverage macro in Fiji, with negative/empty boxes filled in gray. (F) Quantification of number of positive (containing dendrite) 20x20 μm squares.

	Branch order rescue?	Sholl metrics rescue?	Total dendritic length rescue?	Field coverage rescue?
Actn3	Yes	Yes	Yes	Yes
Arp53D	No	Trend	Trend	Yes
CG10177	No	Trend	No	No
CG12620	No	Yes	No	No
CG16716	No	Yes	No	Yes
CG31391	Yes	Yes	No	No
CG32238	No	No	No	No

Figure 3.11 Summary of results.
Summary table of statistically significant rescue of ΔNZK-induced deficits by knockdown of genes of interest.

3.3 Materials and Methods

3.3.1 Drosophila genetics

Drosophila stocks were maintained at 25°C on standard molasses-cornmeal agar. The following strains were obtained from Bloomington *Drosophila* Stock Center and the Vienna Drosophila Resource Center: UAS-RNAi lines directed against targets of interest (see **Appendix** for full listing). Additional strains from other sources included the class IV md neuron reporter strain *GAL4^{477},UAS-mCD8::GFP; ppk1.9-GAL4,UAS-mCD8::GFP*; *UAS-dCBPΔNZK* and *UAS-dCBPΔQ* (Kumar et al. 2004), and *UAS-GMA;GAL4^{477},UAS-Jupiter*::*mCherry*. Detailed

genotypes for each figure are reported in **Table S1**.

3.3.2 Cell isolation and RNA sequencing

Six large-scale magnetic bead cell isolations were performed as previously described (Iyer et al. 2009, Iyer E et al. 2013, Iyer S et al. 2013). Briefly, for each condition 150-200 age-matched third instar larvae expressing *mCD8::GFP* under the control of the class IV *GAL4^{477};ppk1.9-GAL4* driver were collected and washed several times in ddH20. The larvae were then rinsed in RNAse away, ddH20 and coarsely dissected. The tissue was then dissociated to yield single cell suspensions, which were filtered using a 30µm membrane. The filtrate was then incubated with Dynabeads MyOne Streptavidin T1 magnetic beads (Invitrogen) coupled with biotinylated mouse anti-CD8a antibody (eBioscience) for 60 minutes. The md neurons attached to the magnetic beads were then separated using a magnet. The isolated neurons were washed at least five times with PBS to remove any potential non-specific cells and the quality and purity of isolated neurons was assessed under a stereofluorescent microscope equipped with phase contrast for examining the number of fluorescent (GFP-positive) vs. non-fluorescent (GFP-negative) cells. Only if the isolated cells were free of cellular debris and non-specific (i.e. non-fluorescent) contaminants were they retained. The purified class IV neuron populations (ΔNZK, ΔQ, and wild type CIV md neurons) were then lysed and RNA was extracted using Exiqon's miRCURY total RNA isolation kit. Six separate isolations were performed for each condition. The integrity of each RNA sample was assessed using an Agilent 2100 Bioanalyzer and Agilent Technologies RNA Pico Chips, and the three best samples for each condition were selected. RNA quality for these samples was assessed by Beckman-Coulter and all samples were found to be of high quality (FastQC quality scores >30). RNA sequencing was performed by

Beckman-Coulter. RNAseq results from control, ΔQ and ΔNZK CIV samples were then subjected to bioinformatic differential expression analyses. Specifically, the raw read counts provided by Beckman-Coulter were analyzed using the differential expression tools CuffDiff, EdgeR, Gfold and Noiseq (**Fig. 3.4 A**), and the resulting differential expression data was subjected to ontological clustering using DAVID.

3.3.3 Live Imaging Confocal Microscopy, Neuronal Reconstruction, and Morphometric Data Analyses

Live neuronal imaging was performed as previously described (Iyer S et al. 2013, Iyer E et al. 2013) on either a Nikon C1 Plus confocal microscope or a Zeiss LSM780 confocal microscope. Dendritic morphology was quantified as previously described (Iyer E et al. 2013). Briefly, maximum intensity projections of confocal Z-stacks were exported as a jpeg or TIFF. Once exported, images were manually curated to eliminate non-specific auto-fluorescent spots (such as the larval denticle belts) using a custom designed program, *Flyboys* (freely available upon request). For total dendritic length measurements, images were processed and skeletonized in ImageJ (Iyer E et al. 2013, Schneider et al. 2012). Quantitative neuromorphometric information was extracted using the Analyze Skeleton ImageJ plugin and compiled using custom Python algorithms. For Sholl analyses, images were processed using the Sholl plugin for ImageJ (Ferreira et al. 2014). For total dendritic branches and Strahler order, images were reconstructed using NeuronStudio (Wearne et al. 2005). Branch number and order were then extracted using the centripetal branch labeling function. For dendritic field coverage, images were processed using the Internal Coverage macro for ImageJ (Sears and Broihier 2016) using a rectangular ROI bounded by the outermost dendrite on each side, with square side size set to 20 μm.

3.3.4 Statistical Analysis and Data Availability

Statistical analyses of neuromorphometric data and data plotting were performed using GraphPad Prism 7. Error bars reported in the study represent SEM. Statistical analyses were performed using either two-tailed unpaired t-test with Welch's correction or one-way ANOVA using Dunnett's multiple comparisons test when data sets were normally distributed as determined by the Shapiro-Wilk normality test. When data was not normally distributed, appropriate non-parametric tests were used (see **Table S2** for specific tests used in each case). Significance scores indicated on graphs are (*=$p \leq 0.05$, **=$p \leq 0.01$, ***=$p \leq 0.001$). Detailed information on statistical analyses for each figure is reported in Table S2.

4 GENERAL DISCUSSION

4.1 Overview

Neurons utilize a myriad of mechanistic processes to exert regulatory control over cytoskeletal components and thereby ultimately drive neurite morphology (Nanda et al. 2017, Lefebvre and Sanes 2015, Santiago and Bashaw 2014). Proteins that directly impact the stability and/or organization of the cytoskeleton, such as Arp2/3, Formins, MAP2, and Tau, can be degraded at higher or lower rates, sequestered or released from sequestration, or can undergo any of a multitude of post-translational modifications that change their functional properties, such as phosphorylation, glutamylation, glycylation, or acetylation (Georges et al. 2008, Flynn 2013). Additionally, the levels of these proteins present in the neuron can be regulated by transcription factors, which are themselves proteins potentially subject to all the same methods of regulation. This incredible system creates a complex web of interconnected elements that work together and influence each other to finally determine neuronal dendritic morphology. While many pieces of this system have been investigated and described, our understanding of it is by no means complete. Here, we have used the powerful model of the *Drosophila* md sensory neurons to reveal novel mechanisms by which one transcription factor, dCBP, exerts both transcriptional and post-translational effects in order to regulate dendritic morphology.

4.2 Dar1-mediated regulation of dendritic morphology by dCBP

The transcription factor *dar1* has previously been shown to regulate dendritic development of md sensory neurons specifically, without disrupting axonal growth (Ye et al.

2011). *dar1* mutant md neurons display severely reduced arborization whereas Dar1 overexpression promotes dendritic overgrowth in CIV neurons (Ye et al. 2011). Immunohistochemistry analyses suggest that Dar1 protein is localized to the nucleus in all md neuron subclasses (Class I-Class IV) at both embryonic and larval stages of development whereas Dar1 is not expressed in neurons that exhibit mono- or bipolar dendritic morphologies (Ye et al. 2011, Wang et al. 2015). In fact, Dar1 appears to determine multipolar neuron morphology at the level of the dendrite without converting neuronal cell fate (Wang et al. 2015). Cytoskeletal studies in *dar1* gain and loss of function conditions are indicative of a preferential function in regulating microtubules. Genetic interaction studies indicate that Dar1 restricts the expression of the microtubule-severing protein Spastin. Furthermore, microarray analyses of embryonic *dar1* mutant md neurons reveal a transcriptional role for other molecules involved in microtubule-based processes, including several genes encoding Dynein complex components (Wang et al. 2015).

In contrast to these previous studies, we found that Dar1 protein is differentially localized in md neuron classes as development progresses to the third instar larval stage, and that the presence of dCBP in CIV neurons is required to maintain this differential localization, in that RNAi-mediated dCBP knockdown in these neurons results in Dar1 shifting from a predominately cytoplasmic localization to a more nuclear localization pattern while the total amount of Dar1 protein remains unchanged. The basis for the observed differences is as yet unclear, however, it should be noted that the Dar1 antibodies used between our study and the previously published work were independently generated and target different regions of the Dar1 protein, which may account for possible differences in the observed localization patterns. The morphological phenotype induced by dCBP knockdown is distinct in the proliferation of

clustered interstitial dendritic branches that it displays - a phenotype that is also apparent when Dar1 is overexpressed. Because both Dar1 overexpression and dCBP knockdown result in a more nuclear localization of Dar1, it is possible that this morphological phenotype is due to an increase in Dar1-dependent transcriptional regulation. Interestingly, two previous studies revealed that Dar1 appears to function as a transcriptional regulator for microtubule-associated molecules such as Spastin and components of the Dynein complex (Ye et al. 2011, Wang et al. 2015). These findings suggest that increased Dar1 transcriptional regulation may result in a reduction in Spastin-mediated microtubule severing and/or disruptions in Dynein-mediated vesicular transport on microtubules. Either of these regulatory effects could contribute to the morphological defects observed with *dar1* mutants or Dar1 overexpression conditions, because proper balance of neuronal cytoskeletal stability and dynamics is required to maintain the dendritic arbor as well as to initiate new growth. The alterations in the spatial distribution and organization of branching observed in both *dCBP-IR* and Dar1 overexpression are similar to those reported in previous studies that identified roles of Dynein motor complex components, which is intriguing given the role of Dar1 in regulating the expression of genes associated with the Dynein complex. For example, mutations in the *Dynein light intermediate chain* (*Dlic*) gene lead to hyperproliferation of dendritic branches adjacent to the cell body with concomitant stripping of terminal dendritic branching complexity in CIV md neurons (Satoh et al. 2008, Zheng et al. 2008). In another recent study, mutations in the genes *cut up* (*ctp*) and *Cytoplasmic dynein light chain 2* (*Cdlc2*), which both encode cytoplasmic dynein light chains, produced a phenotype that is highly consistent with what is observed with *dCBP* loss-of-function and Dar1 overexpression (i.e. altered spatial distribution of dendritic branching resulting in clustered dendritic tufting at intermediate locations on the dendritic arbor and stripped terminals) (Das et

al. 2017). These findings suggest that different classes of Dynein microtubule motor light chains exert distinct regulatory effects on dendritic branch distribution by potentially contributing to differential regulation of Dynein-linked cargo on microtubules (Das et al. 2017).

Therefore, in the context of dCBP mutant effects on Dar1 protein localization in CIV neurons, the increased nuclear expression of Dar1 observed in *dCBP-IR* CIV neurons may contribute to Dar1 transcriptional effects on Dynein complex components or Spastin, thereby mediating, at least in part, the dendritic defects in the spatial distribution of branches. Such defects could impact the ability to initiate new microtubule-based structures to support growth and branching dynamics, as well as potentially disrupt microtubule-based vesicular transport. Ultimately, additional studies will be required to further characterize the potential mechanistic links between dCBP, Dar1, and microtubule-based processes.

Interestingly, overexpression of Dar1 also results in an increase in both the total amount and the nuclear localization of dCBP. While an in-depth investigation of this phenomenon is outside the scope of these studies, we note that the Dar1 overexpression generated by our *UAS-dar1* transgenic strain is extremely robust. The increase in total dCBP expression could occur through a variety of mechanisms such as via a direct or indirect transcriptional regulatory effect of Dar1 on dCBP expression, by Dar1-mediated stabilization of dCBP expression in CIV neurons or possibly as a homeostatic effect for regulating Dar1 subcellular localization. The increase in nuclear dCBP could potentially occur because the excessive amount of Dar1 present in the nucleus upon overexpression results in dCBP becoming sequestered in the nucleus via interaction with Dar1. Future studies would be necessary in order to distinguish between these possible mechanisms.

Our structure-function studies also support a role for dCBP in determining the subcellular localization of Dar1. In these studies we have demonstrated that expression of either the dCBP-ΔBHQ or dCBP-ΔQ construct results in a significant increase in the nuclear localization of Dar1 in CIV md neurons. These constructs both have deletions of the C-terminal portion of dCBP, but the ΔBHQ construct removes multiple functional domains while the ΔQ construct removes none. However, there is a consensus nuclear export signal (NES) located in the region of dCBP that is removed in the ΔQ, ΔBHQ, and ΔHQ constructs. The sequestration of these three constructs in the nucleus suggests that this sequence is likely a functional NES for dCBP. The ΔHQ construct appears to be expressed at a much lower level than either ΔQ or ΔBHQ (**Fig. 2.9 D, C, E**). While expression of the ΔHQ construct does cause a small but significant increase in nuclear dCBP, it does not appear to be a quantity sufficient to completely out-compete native dCBP in regulating the percent nuclear localization of Dar1, which doubles but does not quite reach significance ($p=0.0652$).

The closest mammalian orthologs of Dar1 are the Krüppel-like transcription factors KLF5 and KLF7 (Ye at al. 2011, Wang et al. 2015, Cox Lab, unpublished results). With respect to neuronal development, KLF7 is required to promote axon and dendrite growth (Laub et al. 2005) and KLF7 overexpression leads to a dramatic increase in the number of primary dendrites in neurons that typically exhibit unipolar or bipolar morphologies, revealing a conserved role of Dar1 and KLF7 in promoting multipolar dendritic arborization profiles (Wang et al. 2015). Interestingly, KLF5 is known to interact with CBP at the N-terminal region of both proteins (Zhang and Teng 2003) and overexpression of KLF5 in cultured retinal ganglion cells results in a modest reduction in neurite growth (Moore et al. 2009), however potential loss-of-function roles for KLF5 in neural development in vertebrates remains unknown. If dCBP and Dar1 interact

similarly then the ΔQ, ΔHQ, and ΔBHQ constructs should preserve this interaction, because they still contain the N-terminal region of dCBP, whereas the ΔNZK and KIX constructs should not be able to interact with Dar1 because neither of them contain the N-terminal region. The results of our structure-function studies support this, as neither the ΔNZK nor KIX constructs cause any change in the percent of Dar1 localized to the nucleus, whereas the three constructs that contain the N-terminal region do, as described above. Moreover, the three constructs that contain the N-terminal domain are also those that lack the putative dCBP NES which may explain how nuclearly localized dCBP serves to promote nuclear sequestration of Dar1.

4.3 Dar1-independent regulation of dendritic morphology by dCBP

The dCBP gain-of-function studies performed here, as well as the structure-function studies, strongly suggest an additional Dar1-independent role for dCBP in the regulation of dendritic morphology. Overexpression of full-length dCBP, while having no discernible effect on the amount or localization of Dar1, causes dramatic defects in CIV dendritic morphology. Expression of the ΔNZK construct likewise has no effect on Dar1 expression or localization, but causes defects in dendritic morphology which appear distinct from the defects caused by full-length overexpression. These observations led us to investigate transcriptional targets of dCBP that could be involved in the regulation of dendritic morphology. Our RNAseq results implied that dCBP engages in both transcriptional activation and repression, but that repression is its predominant role in CIV md neurons. This finding was surprising, because CBP has generally been described and studied as a transcriptional activator (*e.g.* Holmqvist and Mannervik 2013, Valor et al. 2013). We therefore utilized a phenotypic suppression screen approach to identify putative transcriptional targets of dCBP that could be involved in regulation of dendritic

morphology with a focus on putative cytoskeletal regulators and identified several targets that may act in this role. The results from our screen identified a variety of factors associated with different aspects of cytoskeletal regulation for both actin and microtubule based processes and suggest that dCBP-mediated repressive regulation of these factors plays a role in directing normal CIV md sensory neuron dendritogenesis.

4.3.1 Actin-related proteins

Arp53D and Actn3 knockdowns were both effective in rescuing aspects of the ΔNZK-induced morphology deficits. Orthologs of these actin-related proteins are known to be expressed in skeletal muscle, however little is known regarding their potential functional roles in neurons. Arp53D rescued field coverage defects and demonstrated a trend towards rescue of total dendritic length and spatial distribution of branches (as measured by Sholl analysis), while Actn3 demonstrated rescue of all three of these parameters as well as branch order distribution. Both of these proteins are involved in the regulation of actin dynamics, therefore the robustness of the rescue, particularly by Actn3, was somewhat unexpected as we initially hypothesized that microtubule-related effects would be most relevant to rescue of the ΔNZK phenotype.

Actn3 is perhaps best known as a human gene with polymorphisms that have been associated with enhanced athletic performance and is known to be expressed in fast twitch skeletal muscle (Yang et al. 2003). *Drosophila* Actn3 has very little sequence identity with human Actn3, therefore they are unlikely to share many functional properties beyond their calponin homology (CH) domain. Proteins with a single CH domain such as Actn3 are thought to dimerize in order to cross-link actin filaments (Stradal et al. 1998), however single CH domains have also been implicated in microtubule binding in some cases (Hayashi and Ikura 2003).

Because very little is known about the function of Actn3 in *Drosophila*, further investigation of its properties in relation to the neuronal cytoskeleton could be a fruitful path for future research.

Arp53D demonstrates strong (65%) sequence identity with human Gamma-actin, encoded by the *ACTG1* gene. A single previous study in which *Arp53D* was identified in *Drosophila* (Fyrberg et al. 1994) found it to be expressed only in males and predominately in the testes, however there has been no published research on Arp53D since then and our results suggest that it may have some relevance in neuronal cytoskeletal regulation. Gamma-actin is a widely expressed cytoskeletal component in vertebrates (Vandekerckhove and Weber 1978) and Gamma-actin has been shown to bind to both profilin and cofilin (Rainger et al. 2017). The level of sequence identity of Arp53D with Gamma-actin therefore raises the possibility that Arp53D could function as a structural component of the actin cytoskeleton and could perhaps play a role in actin dynamics.

Actin-based structures can range from the highly dynamic, as in the case of actin "waves" that travel along neurites to promote branching (Flynn et al. 2009), to the extremely stable, such as the actin rings that have recently been shown to occur in a periodic manner along the length of many neurites (D'Este et al. 2015). Dendritogenesis requires dynamic actin for growth and pathfinding, as well as more stable actin structures for anchoring and trafficking receptors and other components of the dendrite (Georges et al. 2008). Therefore, hyperactivity of actin binding proteins such as Actn3 may impair dendritic growth by limiting the available pool of dynamic actin, while an overabundance of actin monomers such as Arp53D may inappropriately saturate regulatory factors that maintain homeostatic levels of dynamic vs. stabilized actin, potentially interfering with the actin-mediated growth and branching processes that must occur for dendrites to develop appropriately.

4.3.2 Tubulin polyglutamylases

Knockdown of CG16716, which encodes a tubulin polyglutamylase, rescued field coverage defects and defects in spatial distribution of branches in the ΔNZK phenotype. Another tubulin polyglutamylase, CG32238, was selected from our initial screen because it appeared to rescue some qualitative aspects of ΔNZK morphological defects but it failed to achieve significant rescue for any of the parameters we measured. This failure does not allow us to rule out the possibility that CG32238, or indeed any other genes that did not demonstrate rescue of the ΔNZK phenotype, might be involved in dCBP-mediated regulation of dendritic morphology. It is possible that the knockdown efficiency was insufficient to cause a measurable rescue effect. It is also highly likely that many of the genes we identified by RNAseq function as members of complex pathways and are not individually sufficient to cause a measurable rescue effect.

Tubulin is generally thought of as the more stable of the cytoskeletal components and while this may be broadly accurate, like actin it requires the ability to shift between dynamic and stable states in order to fulfill its many roles in neurons. More stable networks of MTs provide the "roads" on which various cargos are trafficked in the cell body and neurites, as well as providing structural support for existing and developing neurites. More dynamic MTs can depolymerize to provide tubulin dimers for the growth of new MTs or be severed to provide small sections of polymerized tubulin that can then be transported to facilitate MT growth in other areas of the cell. MT stability can be conferred by post-translational modifications (PTMs) and by a variety of MT-associated proteins (MAPs) (Flynn 2013). Whether some specific tubulin PTMs are effectors or consequences of tubulin stability is an area of active scientific research and debate.

Tubulin polyglutamylation is a versatile PTM that can stabilize or destabilize MTs depending on a number of other factors, including the degree of glutamylation present and the presence or absence of various MAPs (Wloga and Gaertig 2010). Polyglutamylation occurs in two steps, initiation and elongation. Some vertebrate tubulin tyrosine ligase-like proteins (TTLLs) are capable of both functions, but TTLL6, the closest vertebrate ortholog of CG16716, is only involved in the elongation step (van Dijk et al. 2007). Overexpression of TTLL6 in *Tetrahymena* (a ciliate model organism) results in MTs that are resistant to nocodazole-induced depolymerization, suggesting that hyperglutamylation exerts a stabilizing effect on these MTs (Wloga et al. 2010). Interestingly, experiments using human cell lines have demonstrated that polyglutamylation by TTLLs that cause the addition of long glutamate side chains (as TTLL6 does) potentiates the activity of the MT severing protein Spastin (Lacroix et al. 2010), which is also one of the transcriptional targets of Dar1 (Ye et al. 2011). The addition of short glutamate side chains, as by TTLL4, did not affect Spastin-mediated MT severing in this study (Lacroix et al. 2010). Thus, it is possible that different degrees of polyglutamylation could directly impact MT stability in neurons. Neurite growth has been shown to be sensitive to the level of Spastin activity, with reductions causing defects in neurite growth, small increases causing increased growth and branching, and abnormally high levels causing severely decreased neurite growth (Riano et al. 2009). If CG16716 functions as TTLL6 does, then increased expression of CG16716 may result in an increase of MT severing by Spastin, which would increase neurite growth to a point and then begin to impair it. This could make dCBP-mediated regulation of polyglutamylation via CG16716 an efficient way to make fine adjustments to neuronal morphology.

4.3.3 Regulators of protein-phosphatase 1 (PP1)

Knockdown of either CG12620 or CG31391 rescues aspects of the ΔNZK-induced defects in spatial branch distribution as measured by Sholl analysis, and knockdown of CG31391 additionally rescues the ΔNZK-induced defects in major and intermediate order dendritic branching. The closest human ortholog of CG12620 is protein-phosphatase inhibitor 2 (PPP1R2) and the closest human ortholog of CG31391 is protein-phosphatase regulatory subunit 36 (PPP1R36). The regulatory subunits of PP1 confer specific substrate recognition, preventing PP1 from dephosphorylating substrates indiscriminately, and can also mediate the localization of PP1 (Virshup and Shenolikar 2009). Various combinations of catalytic and regulatory subunits allow PP1 to modulate cellular functions ranging from cell cycle progression to apoptosis (Cohen 2002). Mammalian PPP1R36 has been shown to promote autophagy during spermatogenesis (Zhang et al. 2016), however since PPP1R36 and CG31391 demonstrate only 23% protein identity we should not draw conclusions from this as to the probable function of CG31391. PPP1R2 has been studied more than PPP1R36 and has been implicated in synaptic scaling (Siddoway et al. 2014) and memory formation processes (Yang et al. 2015) in addition to being studied as a potential regulator of metabolic processes (Permana and Mott 1997). CG12620 has 35% identity with PPP1R2 and so may share some functions, but this would certainly require further study. Although we cannot draw any firm conclusions from current literature as to the specific functions of CG12620 or CG31391, PP1 is known to be an important regulator of many cytoskeletal proteins including tau, MAP1B, and MAP2 (Hoffman et al. 2017), therefore these two regulators of PP1 activity may warrant further investigation in future studies.

4.3.4 Proteins with doublecortin-like kinase activity

Knockdown of CG10177 demonstrated a trend towards rescue of spatial branch distribution as measured by Sholl analysis. CG10177 contains a Doublecortin domain and a calmodulin-dependent kinase (CaM kinase)-like domain. One study using *Drosophila* S2 cells has specifically implicated CG10177 in maintaining proper Golgi organization, however this study was a large-scale screen and did not further investigate CG10177 (Zacharogianni et al. 2011). Doublecortin-like kinases (DCLKs) have been somewhat more extensively studied in mammalian systems however, and doublecortin domains are known to interact directly with MTs and to stabilize them (Gleeson et al. 1999), whereas CaM kinase-like domains have been generally implicated in neuronal development (*e.g.* Won et al. 2006, Kruidering et al. 2001). Intriguingly, DCLKs have been shown to localize specifically to distal dendrites where they promote growth by stabilizing MTs and promote plasticity by inhibiting synapse maturation (Shin et al. 2013). Because overexpression of DCLKs in cultured hippocampal neurons results in increased dendritic growth (Shin et al. 2013), it is not immediately clear how removing transcriptional repression of CG10177 might contribute mechanistically to the ΔNZK phenotype, nor why CG10177 knockdown might mitigate aspects of that phenotype. The large number of genes affected by ΔNZK is likely a confounding factor in this case, and because CG10177 remains an uncharacterized protein in *Drosophila* it is an excellent candidate for further investigation independent of its potential role as a target of dCBP-mediated regulation of dendritic morphology.

4.3.5 Summary and future directions

Many studies have identified CBP as an important factor in disease processes ranging from cancer cell proliferation to some developmental disabilities, however its pleiotropic nature in cellular processes makes it a problematic target in potential treatments (Bordonaro and Lazarova 2015, Valor et al. 2013, Wang et al. 2013). Our research reinforces this, demonstrating that dCBP engages in both transcriptional and post-translational regulation of dendritic development. This regulation occurs via multiple cellular pathways and mechanisms, even when one investigates only the cytoskeletal effects of dCBP-mediated regulation. The identification and characterization of downstream effectors of dCBP-mediated regulation is therefore crucial to the future development of specific treatments for disease processes involving aberrant CBP function. The four types of proteins that we have implicated in dCBP-mediated transcriptional regulation of dendritic development – actin-related proteins, tubulin polyglutamylases, regulators of PP1, and proteins with doublecortin-like kinase activity – each have the potential to be more specific therapeutic targets for disease processes than CBP itself. Further investigation of these downstream effectors of dCBP function will involve more clearly characterizing how they affect cytoskeletal components in md neurons. For example, some tubulin polyglutamylases have been shown to potentiate Spastin activity in human cell lines. To investigate this process in md neuron dendritogenesis we can perform a double knockdown of CG16716 and Spastin, which should exacerbate any phenotype generated by knockdown of CG16716 alone. Alternately, we can knock down CG16716 while overexpressing Spastin. If tubulin polyglutamylation exerts its effects on dendritogenesis via potentiation of Spastin activity, then we will observe a rescue of the CG16716 phenotype under these conditions. These experiments and others like them could

elucidate some of the downstream mechanisms by which dCBP regulates cytoskeletal processes, leading eventually to improvements in pharmaceutical targeting of such processes.

5 SUPPLEMENTAL MATERIAL

Table 1. Genotypes of larvae used in this study.

Figure	Larval Genotypes
2.1	*w^{1118}; $GAL4^{477}$,UAS-mCD8::GFP/+; ppk1.9-GAL4,UAS-mCD8::GFP/+* *w^{1118}; $GAL4^{477}$,UAS-mCD8::GFP/+; ppk1.9-GAL4,UAS-mCD8::GFP/$dar1^{D6}$* *w^{1118}, $elav^{C155}$-GAL4, UAS-mCD8::GFP, hsFLP; +; FRT80B, $dar1^{D6}$* (MARCM) *w^{1118}; $GAL4^{477}$,UAS-mCD8::GFP/+; ppk1.9-GAL4,UAS-mCD8::GFP/UAS-dar1*
2.2 A	*w^{1118}; $GAL4^{477}$,UAS-mCD8::GFP/+; ppk1.9-GAL4,UAS-mCD8::GFP/+*
2.2 B	*w^{1118}; +; +* *w^{1118}; +; PBac(WH)$dar1^{f01014}$*
2.3	*w^{1118}; $GAL4^{477}$,UAS-mCD8::GFP/+; ppk1.9-GAL4,UAS-mCD8::GFP/+* *w^{1118}; $GAL4^{477}$,UAS-mCD8::GFP/+; ppk1.9-GAL4,UAS-mCD8::GFP/UAS-$nej^{RNAi(HMS01507)}$* *w^{1118}; $GAL4^{477}$,UAS-mCD8::GFP/+; ppk1.9-GAL4,UAS-mCD8::GFP/UAS-nej.wt-V5*
2.4	*w^{1118}; +; +*
2.5	*w^{1118}; $GAL4^{477}$,UAS-mCD8::GFP/+; ppk1.9-GAL4,UAS-mCD8::GFP/+* *w^{1118}; $GAL4^{477}$,UAS-mCD8::GFP/+; ppk1.9-GAL4,UAS-mCD8::GFP/UAS-$nej^{RNAi(HMS01507)}$* *w^{1118}; $GAL4^{477}$,UAS-mCD8::GFP/+; ppk1.9-GAL4,UAS-mCD8::GFP/UAS-dar1*
2.6	*w^{1118}; $GAL4^{477}$,UAS-mCD8::GFP/+; ppk1.9-GAL4,UAS-mCD8::GFP/+* *w^{1118}; $GAL4^{477}$,UAS-mCD8::GFP/+; ppk1.9-GAL4,UAS-mCD8::GFP/UAS-nej.wt-V5* *w^{1118}; $GAL4^{477}$,UAS-mCD8::GFP/+; ppk1.9-GAL4,UAS-mCD8::GFP/UAS-dar1*
2.7-2.9	*w^{1118}; $GAL4^{477}$,UAS-mCD8::GFP/+; ppk1.9-GAL4,UAS-mCD8::GFP/+* *w^{1118}; $GAL4^{477}$,UAS-mCD8::GFP/UAS-dCBP KIX; ppk1.9-GAL4,UAS-mCD8::GFP/+* *w^{1118}; $GAL4^{477}$,UAS-mCD8::GFP/UAS-dCBPΔBHQ; ppk1.9-GAL4,UAS-mCD8::GFP/+* *w^{1118}; $GAL4^{477}$,UAS-mCD8::GFP/+; ppk1.9-GAL4,UAS-mCD8::GFP/UAS-dCBPΔHQ* *w^{1118}; $GAL4^{477}$,UAS-mCD8::GFP/UAS-nej.F2161A-V5; ppk1.9-GAL4,UAS-mCD8::GFP/+* *w^{1118}; $GAL4^{477}$,UAS-mCD8::GFP/UAS-dCBPΔNZK; ppk1.9-GAL4,UAS-mCD8::GFP/+* *w^{1118}; $GAL4^{477}$,UAS-mCD8::GFP/UAS-dCBPΔQ; ppk1.9-GAL4,UAS-mCD8::GFP/+* *P(GSV1)nej^{S-20}/+; $GAL4^{477}$,UAS-mCD8::GFP/+; ppk1.9-GAL4,UAS-mCD8::GFP/+*
3.2	*UAS-GMA/+;$GAL4^{477}$,UAS-mCherry::Jup/+; +* *UAS-GMA/+;$GAL4^{477}$,UAS-mCherry::Jup/UAS-dCBPΔNZK; +* *UAS-GMA/+;$GAL4^{477}$,UAS-mCherry::Jup/UAS-dCBPΔQ; +*

3.5-3.9	*w^{1118}; +; ppk1.9-GAL4,UAS-mCD8::GFP/+* *w^{1118}; UAS-dCBPΔNZK/UAS-mCD8::RFP; ppk1.9-GAL4,UAS-mCD8::GFP/+* *w^{1118}; UAS-dCBPΔNZK/+; ppk1.9-GAL4,UAS-mCD8::GFP/Arp53D$^{RNAi(HMS02876)}$* *w^{1118}; UAS-dCBPΔNZK/+; ppk1.9-GAL4,UAS-mCD8::GFP/CG10177$^{RNAi(HMC04182)}$* *w^{1118}; UAS-dCBPΔNZK/CG32238$^{RNAi(HMJ21441)}$; ppk1.9-GAL4,UAS-mCD8::GFP/+* *w^{1118}; UAS-dCBPΔNZK/+; ppk1.9-GAL4,UAS-mCD8::GFP/Actn3$^{RNAi(JF02279)}$* *w^{1118}; UAS-dCBPΔNZK/CG12620$^{RNAi(KK103350)}$; ppk1.9-GAL4,UAS-mCD8::GFP/+* *w^{1118}; UAS-dCBPΔNZK/CG31391$^{RNAi(HMJ24131)}$; ppk1.9-GAL4,UAS-mCD8::GFP/+* *w^{1118}; UAS-dCBPΔNZK/CG16716$^{RNAi(HMJ23972)}$; ppk1.9-GAL4,UAS-mCD8::GFP/+*

Table 2. Statistics by figure.

Figure/Label	Passed Shapiro-Wilk Normality?	Statistical tests used	p-value	N value (neurons)
Fig. 2.3 D		One-way ANOVA with Tukey's multiple comparisons test		
WT	Yes			11
dCBP-IR	Yes		<0.0001	12
dCBP OE	Yes		<0.0001	14
Fig. 2.3 E		One-way ANOVA with Tukey's multiple comparisons test		
WT	Yes			8
dCBP-IR	Yes		0.0001	10
dCBP OE	Yes		<0.0001	11
Fig. 2.3 F		One-way ANOVA with Tukey's multiple comparisons test		
WT	Yes			8
dCBP-IR	Yes		<0.0001	10
dCBP OE	Yes		<0.0001	11
Fig. 2.3 H 1st order		Two-way ANOVA with Dunnett's multiple comparisons test		
WT	Yes			9
dCBP-IR	Yes		0.9929	10
dCBP OE	Yes		0.9990	11
Fig. 2.3 H 2nd order		Two-way ANOVA with Dunnett's multiple comparisons test		
WT	Yes			9
dCBP-IR	Yes		0.9809	10
dCBP OE	Yes		0.9933	11
Fig. 2.3 H 3rd order		Two-way ANOVA with Dunnett's multiple comparisons test		
WT	Yes			9
dCBP-IR	Yes		0.8994	10
dCBP OE	Yes		0.9646	11
Fig. 2.3 H 4th order		Two-way ANOVA with Dunnett's multiple comparisons test		
WT	Yes			9
dCBP-IR	Yes		0.3551	10

dCBP OE	Yes		0.9721	11
Fig. 2.3 H 5th order		Two-way ANOVA with Dunnett's multiple comparisons test		
WT	Yes			9
dCBP-IR	Yes		0.0005	10
dCBP OE	Yes		0.0001	11
Fig. 2.3 H 6th order		Two-way ANOVA with Dunnett's multiple comparisons test		
WT	Yes			9
dCBP-IR	Yes		0.0001	10
dCBP OE	Yes		0.0001	11
Fig. 2.4 G		Unpaired t test with Welch's correction		
CI	Yes			9
CIV	Yes		0.0002	10
Fig. 2.4 H		Unpaired t test with Welch's correction		
CI	Yes			10
CIV	Yes		0.6586	10
Fig. 2.4 I		Unpaired t test with Welch's correction		
CI	Yes			9
CIV	Yes		<0.0001	10
Fig. 2.4 J		Unpaired t test with Welch's correction		
CI	Yes			9
CIV	Yes		<0.0001	10
Fig. 2.5 D		Unpaired t test with Welch's correction		
WT	Yes			14
dCBP-IR	Yes		0.7006	12
Fig. 2.5 E		Unpaired t test with Welch's correction		
WT	Yes			14
dCBP-IR	Yes		<0.0001	12
Fig. 2.5 G		One-way ANOVA with Tukey's multiple comparisons test		
WT	Yes			9
dar1 OE	Yes		0.0006 (vs. WT)	11
dCBP-IR	Yes		0.0011 (vs. WT) 0.9969 (vs. Dar1 OE)	8
Fig. 2.5 H		One-way ANOVA with		

		Tukey's multiple comparisons test		
WT	Yes			10
dar1 OE	Yes		0.0006 (vs. WT)	12
dCBP-IR	Yes		0.0001 (vs. WT) 0.5167 (vs. Dar1 OE)	8
Fig. 2.6 J		Unpaired t-test with Welch's correction		
WT	Yes			12
dCBP OE	Yes		0.1028	6
Fig. 2.6 K		Unpaired t-test with Welch's correction		
WT	Yes			14
dar1 OE	Yes		<0.0001	16
Fig. 2.6 L		Unpaired t-test with Welch's correction		
WT	Yes			12
dCBP OE	Yes		0.1998	6
Fig. 2.6 M		Unpaired t-test with Welch's correction		
WT	Yes			15
dar1 OE	Yes		<0.0001	16
Fig. 2.8 A		Kruskal-Wallis test with Dunn's multiple comparisons test		
WT	Yes			11
dCBP-KIX	Yes		>0.9999	9
dCBP-ΔNZK	Yes		0.0102	9
dCBP-ΔBHQ	Yes		>0.9999	11
dCBP-ΔHQ	No		>0.9999	9
dCBP-ΔQ	Yes		<0.0001	8
dCBP-ΔH	Yes		0.0195	11
$dCBP^{S-20}$	Yes		<0.0001	12
Fig. 2.8 B		One-way ANOVA with Dunnett's multiple comparisons test		
WT	Yes			8
dCBP-KIX	Yes		0.4268	9
dCBP-ΔNZK	Yes		0.0001	9
dCBP-ΔBHQ	Yes		0.0001	10
dCBP-ΔHQ	Yes		0.0001	9
dCBP-ΔQ	Yes		0.0001	9
dCBP-ΔH	Yes		0.0001	11
$dCBP^{S-20}$	Yes		0.0001	12
Fig. 2.8 C		Kruskal-Wallis test with		

		Dunn's multiple comparisons test		
WT	Yes			8
dCBP-KIX	Yes		>0.9999	9
dCBP-ΔNZK	Yes		0.9515	9
dCBP-ΔBHQ	Yes		0.0050	11
dCBP-ΔHQ	No		0.0645	8
dCBP-ΔQ	No		<0.0001	9
dCBP-ΔH	Yes		0.0046	10
$dCBP^{S-20}$	Yes		<0.0001	12
Fig. 2.8 D		One-way ANOVA with Dunnett's multiple comparisons test		
WT	Yes			9
dCBP-KIX	Yes		0.3528	10
dCBP-ΔNZK	Yes		0.0001	9
dCBP-ΔBHQ	Yes		0.5918	11
dCBP-ΔHQ	Yes		0.9978	9
dCBP-ΔQ	Yes		0.0001	8
dCBP-ΔH	Yes		0.0001	10
$dCBP^{S-20}$	Yes		0.0001	11
Fig. 2.8 E 1st order		Two-way ANOVA with Dunnett's multiple comparisons test		
WT	Yes			9
dCBP-KIX	Yes		0.9996	10
dCBP-ΔNZK	Yes		0.8674	9
dCBP-ΔBHQ	Yes		0.8510	11
dCBP-ΔHQ	Yes		0.8674	9
dCBP-ΔQ	Yes		0.5976	9
dCBP-ΔH	Yes		0.8954	11
$dCBP^{S-20}$	Yes		0.9999	12
Fig. 2.8 E 2nd order		Two-way ANOVA with Dunnett's multiple comparisons test		
WT	Yes			9
dCBP-KIX	Yes		0.9995	10
dCBP-ΔNZK	Yes		0.2310	9
dCBP-ΔBHQ	Yes		0.4048	11
dCBP-ΔHQ	Yes		0.5251	9
dCBP-ΔQ	Yes		0.0365	9
dCBP-ΔH	Yes		0.6455	11
$dCBP^{S-20}$	Yes		0.9997	12
Fig. 2.8 E 3rd order		Two-way ANOVA with Dunnett's multiple		

		comparisons test		
WT	Yes			9
dCBP-KIX	Yes		0.8292	10
dCBP-ΔNZK	Yes		0.0001	9
dCBP-ΔBHQ	Yes		0.0001	11
dCBP-ΔHQ	Yes		0.0001	9
dCBP-ΔQ	Yes		0.0001	9
dCBP-ΔH	Yes		0.0003	11
$dCBP^{S-20}$	Yes		0.9806	12
Fig. 2.8 E 4th order		Two-way ANOVA with Dunnett's multiple comparisons test		
WT	Yes			9
dCBP-KIX	Yes		0.9975	10
dCBP-ΔNZK	Yes		0.5620	9
dCBP-ΔBHQ	Yes		0.5124	11
dCBP-ΔHQ	Yes		0.7371	9
dCBP-ΔQ	Yes		0.0319	9
dCBP-ΔH	Yes		0.6174	11
$dCBP^{S-20}$	Yes		0.8542	12
Fig. 2.8 E 5th order		Two-way ANOVA with Dunnett's multiple comparisons test		
WT	Yes			9
dCBP-KIX	Yes		0.7365	10
dCBP-ΔNZK	Yes		0.0001	9
dCBP-ΔBHQ	Yes		0.0001	11
dCBP-ΔHQ	Yes		0.0001	9
dCBP-ΔQ	Yes		0.0001	9
dCBP-ΔH	Yes		0.0001	11
$dCBP^{S-20}$	Yes		0.0001	12
Fig. 2.8 E 6th order		Two-way ANOVA with Dunnett's multiple comparisons test		
WT	Yes			9
dCBP-KIX	Yes		0.0575	10
dCBP-ΔNZK	Yes		0.0001	9
dCBP-ΔBHQ	Yes		0.0001	11
dCBP-ΔHQ	Yes		0.0001	9
dCBP-ΔQ	Yes		0.0001	9
dCBP-ΔH	Yes		0.0001	11
$dCBP^{S-20}$	Yes		0.0001	12
Fig. 2.9 A dCBP		Kruskal-Wallis test with Dunn's multiple comparisons test		

WT	No			18
dCBP-KIX	Yes		>0.9999	20
Fig. 2.9 A dar1		Kruskal-Wallis test with Dunn's multiple comparisons test		
WT	Yes			18
dCBP-KIX	Yes		>0.9999	19
Fig. 2.9 B dCBP		Kruskal-Wallis test with Dunn's multiple comparisons test		
WT	No			18
dCBP-ΔNZK	Yes		>0.9999	22
Fig. 2.9 B dar1		Kruskal-Wallis test with Dunn's multiple comparisons test		
WT	Yes			18
dCBP-ΔNZK	No		>0.9999	22
Fig. 2.9 C dCBP		Kruskal-Wallis test with Dunn's multiple comparisons test		
WT	No			18
dCBP-ΔBHQ	Yes		0.0009	30
Fig. 2.9 C dar1		Kruskal-Wallis test with Dunn's multiple comparisons test		
WT	Yes			18
dCBP-ΔBHQ	Yes		0.0008	29
Fig. 2.9 D dCBP		Kruskal-Wallis test with Dunn's multiple comparisons test		
WT	No			18
dCBP-ΔHQ	Yes		0.0408	16
Fig. 2.9 D dar1		Kruskal-Wallis test with Dunn's multiple comparisons test		
WT	Yes			18
dCBP-ΔHQ	Yes		0.0652	17
Fig. 2.9 E dCBP		Kruskal-Wallis test with Dunn's multiple comparisons test		
WT	No			18
dCBP-ΔQ	Yes		<0.0001	31
Fig. 2.9 E dar1		Kruskal-Wallis test with Dunn's multiple comparisons test		

WT	Yes			18
dCBP-ΔQ	Yes		<0.0001	32
Fig. 3.6 A		One-way ANOVA with Dunnett's multiple comparisons test		
WT	Yes			9
ΔNZK	Yes		0.0163	11
Arp53D-IR	Yes		0.3106	8
CG10177-IR	Yes		0.9999	10
CG32238-IR	Yes		0.1464	8
Actn3-IR	Yes		0.1458	10
CG12620-IR	Yes		0.6860	10
CG31391-IR	Yes		0.0185	6
CG16716-IR	Yes		0.9996	7
Fig. 3.6 B		One-way ANOVA with Dunnett's multiple comparisons test		
WT	Yes			8
ΔNZK	Yes		0.0022	11
Arp53D-IR	Yes		0.1911	7
CG10177-IR	Yes		0.9869	10
CG32238-IR	Yes		0.0037	9
Actn3-IR	Yes		0.0017	10
CG12620-IR	Yes		0.0793	10
CG31391-IR	Yes		0.0193	7
CG16716-IR	Yes		0.5327	6
Fig. 3.7 A		One-way ANOVA with Dunnett's multiple comparisons test		
WT	Yes			8
ΔNZK	Yes		0.0001	11
Arp53D-IR	Yes		0.4751	8
CG10177-IR	Yes		0.0598	10
CG32238-IR	Yes		0.1263	10
Actn3-IR	Yes		0.0060	9
CG12620-IR	Yes		0.1330	10
CG31391-IR	Yes		0.0026	7
CG16716-IR	Yes		0.0114	8
Fig. 3.7 B		One-way ANOVA with Dunnett's multiple comparisons test		
WT	Yes			9
ΔNZK	Yes		0.0001	12
Arp53D-IR	Yes		0.0889	8
CG10177-IR	Yes		0.8266	10

CG32238-IR	Yes		0.9996	10
Actn3-IR	Yes		0.1076	10
CG12620-IR	Yes		0.0250	10
CG31391-IR	Yes		0.9724	7
CG16716-IR	Yes		0.0742	8
Fig. 3.8 A		One-way ANOVA with Dunnett's multiple comparisons test		
WT	Yes			9
ΔNZK	Yes		0.0005	12
Arp53D-IR	Yes		0.0553	8
CG10177-IR	Yes		0.9252	10
CG32238-IR	Yes		0.1313	10
Actn3-IR	Yes		0.0392	10
CG12620-IR	Yes		0.9996	10
CG31391-IR	Yes		0.9911	7
CG16716-IR	Yes		0.9739	8
Fig. 3.8 B		Unpaired t test with Welch's correction		
WT	Yes			8
ΔNZK	Yes		0.7573	10
Fig. 3.9 F		One-way ANOVA with Dunnett's multiple comparisons test		
WT	Yes			9
ΔNZK	Yes		0.0001	12
Arp53D-IR	Yes		0.0005	8
CG10177-IR	Yes		0.2889	9
CG32238-IR	Yes		0.8154	10
Actn3-IR	Yes		0.0001	10
CG12620-IR	Yes		0.1702	10
CG31391-IR	Yes		0.9928	7
CG16716-IR	Yes		0.0246	7

REFERENCES

Aizawa H, Hu SC, Bobb K, Balakrishnan K, Ince G, Gurevich I, Cowan M, Ghosh A. 2004. Dendrite development regulated by CREST, a calcium-regulated transcriptional activator. Science Jan 9;303(5655):197-202.

Akimaru H, Chen Y, Dai P, Hou DX, Nonaka M, Smolik SM, Armstrong S, Goodman RH, Ishii S. 1997. Drosophila CBP is a co-activator of cubitus interruptus in hedgehog signalling. Nature Apr 17;386(6626):735-8.

Andersen EF, Asuri NS, Halloran MC. 2011. In Vivo Imaging of Cell Behaviors and F-Actin Reveals LIM-HD Transcription Factor Regulation of Peripheral versus Central Sensory Axon Development. Neural Development 6(1): 27.

Anderton BH, Callahan L, Coleman P, Davies P, Flood D, Jicha GA, Ohm T, Weaver C. 1998. Dendritic changes in Alzheimer's disease and factors that may underlie these changes. Prog Neurobiol 55(6):595–609.

Bellen HJ, Tong C, Tsuda H. 2010. 100 years of Drosophila research and its impact on vertebrate neuroscience: a history lesson for the future. Nat Rev Neurosci 11:514-522.

Belmonte MK, Allen G, Beckel-Mitchener A, Boulanger LM, Carper RA, Webb SJ. 2004. Autism and abnormal development of brain connectivity. J Neurosci 24(42):9228-31.

Bordonaro M, Lazarova DL. 2015. CREB-binding protein, p300, butyrate, and Wnt signaling in colorectal cancer. World J Gastroenterol Jul21;21(27):8238-48.

Chatterjee S, Mizar P, Cassel R, Neidl R, Selvi BR, Mohankrishna DV, Vedamurthy BM, Schneider A, Bousiges O, Mathis C, Cassel JC, Eswaramoorthy M, Kundu TK, Boutillier AL. 2013. A novel activator of CBP/p300 acetyltransferases promotes neurogenesis and extends memory duration in adult mice. J Neurosci. Jun 26;33(26):10698-712.

Chiang AS, Lin CY, Chuang CC, Chang HM, Hsieh CH, Yeh CW, Shih CT, Wu JJ, Wang GT, Chen YC, Wu CC, Chen GY, Ching YT, Lee PC, Lin CY, Lin HH, Wu CC, Hsu HW, Huang YA, Chen JY, Chiang HJ, Lu CF, Ni RF, Yeh CY, Hwang JK. 2011. Three-dimensional reconstruction of brain-wide wiring networks in Drosophila at single-cell resolution. Curr Biol 21:1–11.

Chrivia JC, Kwok RP, Lamb N, Hagiwara M, Montminy MR, Goodman RH. 1993. Phosphorylated CREB binds specifically to the nuclear protein CBP. Nature 365: 855-859.

Cohen PT. 2002. Protein phosphatase 1--targeted in many directions. J Cell Sci. Jan 15;115(Pt 2):241-56.

Copf T. 2015. Importance of gene dosage in controlling dendritic arbor formation during development. Eur J Neurosci Sep;42(6):2234-49.

Cortés-Mendoza J, Diaz de León-Guerrero SD, Pedraza-Alva G, Pérez-Martínez L. 2013. Shaping synaptic plasticity: The role of activity-mediated epigenetic regulation on gene transcription. Int J Dev Neurosci 31(6):359-69.

Couton L, Mauss AS, Yunusov T, Diegelmann S, Evers JF, Landgraf, M. 2015. Development of connectivity in a motoneuronal network in Drosophila larvae. Curr Biol 25:568-576.

Crozatier M, Vincent A. 2008. Control of multidendritic neuron differentiation in Drosophila: the role of Collier. Dev Biol 315(1):232-42.

D'Este E, Kamin D, Göttfert F, El-Hady A, Hell SW. 2015. STED nanoscopy reveals the ubiquity of subcortical cytoskeleton periodicity in living neurons. Cell Rep. Mar 3;10(8):1246-51

Das R, Bhattacharjee S, Patel AA, Harris JM, Bhattacharya S, Letcher JM, Clark SG, Nanda S, Iyer EPR, Ascoli GA, Cox DN. 2017. Dendritic Cytoskeletal Architecture Is Modulated by Combinatorial Transcriptional Regulation in Drosophila melanogaster. Genetics Dec;207(4):1401-1421.

de la Torre-Ubieta L, Bonni A. 2011. Transcriptional regulation of neuronal polarity and morphogenesis in the mammalian brain. Neuron 72:22-40.

Dickson DW, Liu W, Hardy J, Farrer M, Mehta N, Uitti R, Mark M, Zimmerman T, Golbe L, Sage J, Sima A, D'Amato C, Albin R, Gilman S, Yen SH. 1999. Widespread alterations of alpha-synuclein in multiple system atrophy. Am J Path 155(4):1241-51.

Feng J, Yan Z, Ferreira A, Tomizawa K, Liauw JA, Zhuo M, Allen PB, Ouimet CC and Greengard P. 2000. Spinophilin regulates the formation and function of dendritic spines. Proc Natl Acad Sci USA Aug 1;97(16):9287-92.

Ferreira T, Ou Y, Li S, Giniger E, van Meyel DJ. 2014. Dendrite architecture organized by transcriptional control of the F-actin nucleator Spire. Development 141(3):650-60.

Fiala JC, Spacek J, Harris KM. 2002. Dendritic spine pathology: cause of consequence of neurological disorders? Brain Res Rev 39(1):29-54.

Flynn KC, Pak CW, Shaw AE, Bradke F, Bamburg JR. 2009. Growth cone-like waves transport actin and promote axonogenesis and neurite branching. Dev Neurobiol. Oct;69(12):761-79.

Flynn KC. 2013. The cytoskeleton and neurite initiation. Bioarchitecture. Jul-Aug;3(4):86-109.

Fyrberg C, Ryan L, Kenton M, Fyrberg E. 1994. Genes encoding actin-related proteins of Drosophila melanogaster. J Mol Biol. Aug 19;241(3):498-503.

Gemayel R, Chavali S, Pougach K, Legendre M, Zhu B, Boeynaems S, van der Zande E, Gevaert K, Rousseau F, Schymkowitz J, Babu MM, Verstrepen KJ. 2015. Variable Glutamine-Rich Repeats Modulate Transcription Factor Activity. Mol Cell Aug 20;59(4):615-27.

Georges PC, Hadzimichalis NM, Sweet ES, Firestein BL. 2008. The yin-yang of dendrite morphology: unity of actin and microtubules. Mol Neurobiol. Dec;38(3):270-84.

Gleeson JG, Lin PT, Flanagan LA, Walsh CA. 1999. Doublecortin is a microtubule-associated protein and is expressed widely by migrating neurons. Neuron. Jun;23(2):257-71.

Grueber WB, Jan LY and Jan YN. 2002. Tiling of the Drosophila epidermis by multidendritic sensory neurons. Development Jun; 129(12):2867-78.

Grueber WB, Jan LY and Jan YN. 2003. Different levels of the homeodomain protein cut regulate distinct dendrite branching patterns of Drosophila multidendritic neurons. Cell Mar 21; 112(6):805-18.

Hand R, Bortone D, Mattar P, Nguyen L, Heng JI, Guerrier S, Boutt E, Peters E, Barnes AP, Parras C, Schuurmans C, Guillemot F, Polleux F. 2005. Phosphorylation of Neurogenin2 Specifies the Migration Properties and the Dendritic Morphology of Pyramidal Neurons in the Neocortex. Neuron 48 (1): 45–62.

Hattori Y, Sugimura K, Uemura T. 2007. Selective expression of Knot/Collier, a transcriptional regulator of the EBF/Olf-1 family, endows the Drosophila sensory system with neuronal class-specific elaborated dendritic patterns. Genes Cells 12(9)1011-22.

Hattori Y, Usui T, Satoh D, Moriyama S, Shimono K, Takehiko I, Shirahige K, Uemura T. 2013. Sensory-neuron subtype-specific transcriptional programs controlling dendrite morphogeneis: genome-wide analysis of Abrupt and Knot/Collier. Dev Cell 27(5):530-44.

Hayashi I, Ikura M. 2003. Crystal structure of the amino-terminal microtubule-binding domain of end-binding protein 1 (EB1). J Biol Chem. Sep 19;278(38):36430-4.

Helmstaedter M, Mitra P. 2012. Computational Methods and Challenges for Large-Scale Circuit Mapping. Curr Opin Neurobiol 22(1):162-9.

Hoffman A, Taleski G, Sontag E. 2017. The protein serine/threonine phosphatases PP2A, PP1 and calcineurin: A triple threat in the regulation of the neuronal cytoskeleton. Mol Cell Neurosci. Oct;84:119-131.

Holmqvist PH, Mannervik M. 2013. Genomic occupancy of the transcriptional co-activators p300 and CBP. Transcription Jan-Feb;4(1):18-23

Honjo K, Mauthner SE, Wang Y, Skene JHP, Tracey Jr WD. 2016. Nociceptor-enriched genes required for normal thermal nociception. Cell Reports, 16(2), 295-303.

Iyer EPR, Iyer SC, Sulkowski MJ, Cox DN. 2009. Isolation and purification of *Drosophila* peripheral neurons by magnetic bead sorting. J Vis Exp (34), e1599.

Iyer SC, Wang D, Iyer EPR, Trunnell SA, Meduri R, Shinwari R, Sulkowski MJ, Cox DN. 2012. The RhoGEF Trio functions in sculpting class specific dendrite morphogenesis in Drosophila sensory neurons. PLoS ONE 7(3):e33634.

Iyer SC, Iyer EPR, Meduri R, Rubaharan M, Kuntimaddi A, Karamsetty M, Cox DN. 2013b. Cut, via CrebA, transcriptional regulates the COPII secretory pathway to direct dendrite development in Drosophila. J Cell Sci 126(20):4732-45.

Iyer EPR, Iyer SC, Sullivan L, Wang D, Meduri R, Graybeal LL, Cox DN. 2013a. Functional genomic analyses of two morphologically distinct classes of *Drosophila* sensory neurons: post-mitotic roles of transcription factors in dendritic patterning. PLoS ONE 8(8): e72434.

Jagadha V, Becker LE. 1988. Brain morphology in Duchenne Muscular Dystrophy: A Golgi study. Pediatric Neurology 4(2):87-92.

Jan YN, Jan LY. 2010. Branching out: mechanisms of dendritic arborization. Nat Rev Neurosci 11:316-328.

Jinushi-Nakao S, Arvind R, Amikura R, Kinameri E, Liu AW, Moore AW. 2007. Knot/Collier and cut control different aspects of dendrite cytoskeleton and synergize to define final arbor shape. Neuron Dec 20; 56(6):963-78.

Kamei Y, Xu L, Heinzel T, Torchia J, Kurokawa R, Gloss B, ... & Rosenfeld MG. 1996. A CBP integrator complex mediates transcriptional activation and AP-1 inhibition by nuclear receptors. Cell, 85(3), 403-414.

Kaufmann WE, Moser HW. 2000. Dendritic anomalies in disorders associated with mental retardation. Cerebral Cortex 10(10):981-91.

Kim MD, Jan LY, Jan YN. 2006. The bHLH-PAS protein Spineless is necessary for the diversification of dendrite morphology of Drosophila dendritic arborization neurons. Genes Dev 20(20):2806-19.

Kirilly D, Wong JJ, Lim EK, Wang Y, Zhang H, Wang C, Liao Q, Wang H, Liou YC, Wang H, Yu F. 2011. Intrinsic epigenetic factors cooperate with the steroid hormone ecdysone to govern dendrite pruning in Drosophila. Neuron Oct 6;72(1):86-100.

Kruidering M, Schouten T, Evan GI, Vreugdenhil E. 2001. Caspase-mediated cleavage of the Ca2+/calmodulin-dependent protein kinase-like kinase facilitates neuronal apoptosis. J Biol Chem. Oct 19;276(42):38417-25.

Kulkarni VA, Firestein BL. 2012. The dendritic tree and brain disorders. Mol Cell Neurosci 50:10-20.

Kumar JP, Jamal T, Doetsch A, Turner FR, Duffy JB. 2004. CREB Binding Protein Functions during Successive Stages of Eye Development in Drosophila. Genetics 168(2):877-93.

Laity JH, Lee BM, Wright PE. 2001. Zinc finger proteins: new insights into structural and functional diversity. Curr Opin Struct Biol 11(1):39-46.

Lacroix B, van Dijk J, Gold ND, Guizetti J, Aldrian-Herrada G, Rogowski K, Gerlich DW, Janke C. 2010. Tubulin polyglutamylation stimulates spastin-mediated microtubule severing. J Cell Biol. Jun 14;189(6):945-54.

Laub F, Lei L, Sumiyoshi H, Kajimura D, Dragomir C, Smaldone S, Puche AC, Petros TJ, Mason C, Parada LF, Ramirez F. 2005. Transcription factor KLF7 is important for neuronal morphogenesis in selected regions of the nervous system. Mol. Cell Biol. 25: 5699-5711.

Lefebvre JL, Sanes JR, Kay JN. 2015. Development of dendritic form and function. Annu Rev Cell Dev Biol 31:741-77.

Li J, Sutter C, Parker DS, Blauwkamp T, Fang M, Cadigan KM. 2007. CBP/p300 are bimodal regulators of Wnt signaling. EMBO J May2;26(9):2284-94

Li W, Wang F, Menut L, Gao FB. 2004. BTB/POZ-Zinc finger protein Abrupt suppresses dendritic branching in a neuronal subtype-specific and dosage-dependent manner. Neuron 43(6):823-34.

Moore AW, Jan LY, Jan YN. 2002. Hamlet, a binary genetic switch between single- and multiple-dendritic neuron morphology. Science 297:1355-58.

Moore DL, Blackmore MG, Hu Y, Kaestner KH, Bixby JL, Lemmon VP, Goldberg JL. 2009. KLF family members regulate intrinsic axon regeneration ability. Science 326:298-301.

Mukherjee SP, Behar M, Birnbaum HA, Hoffman A, Wright PE, Ghosh G. 2013. Analysis of the RelA:CBP/p300 interaction reveals its involvement in NF-κB-driven transcription. PLoS Biol Sep;11(9):e1001647.

Nagel JC, Delandre Y, Zhang F, Forstner F, Moore AW, Tavosanis G. 2012. Fascin controls neuronal class-specific dendrite arbor morphology. Development 139(16):2999-3009.

Nanda S, Das R, Cox DN, and Ascoli GA. 2017. Structural plasticity in dendrites: developmental neurogenetics, morphological reconstructions, and computational modeling, pp. 1-34 in Neurobiological and Psychological Aspects of Brain Recovery, edited by L. Petrosini, Springer Press, Cham.

Permana PA, Mott DM. 1997. Genetic analysis of human type 1 protein phosphatase inhibitor 2 in insulin-resistant Pima Indians. Genomics Apr 1;41(1):110-4.

Petrij F, Giles RH, Dauwerse HG, Saris JJ, Hennekam, RC, Masuno M, Tommerup N, van Ommen GJ, Goodman RH, Peters DJ et al. 1995. Rubinstein-Taybi syndrome caused by mutations in the transcriptional co-activator CBP. Nature 376(6538):348-51.

Puram SV, Bonni A. 2013. Cell-intrinsic drivers of dendrite morphogenesis. Development 140:4657-4671.

Rainger J, Williamson KA, Soares DC, Truch J, Kurian D, Gillessen-Kaesbach G, Seawright A, Prendergast J, Halachev M, Wheeler A, McTeir L, Gill AC, van Heyningen V, Davey MG; UK10K, FitzPatrick DR. 2017. A recurrent de novo mutation in ACTG1 causes isolated ocular coloboma. Hum Mutat Aug;38(8):942-946.

Ramocki MB, Zoghbi, HY. 2008. Failure of neuronal homeostasis results in common neuropsychiatric phenotypes. Nature 455:912-918.

Redmond L, Kashani AH, Ghosh A. 2002. Calcium regulation of dendritic growth via CaM kinase IV and CREB-mediated transcription. Neuron Jun 13;34(6):999-1010.

Reiter LT, Potocki L, Chien S, Gribskov M, Bier E. 2001. A systematic analysis of human disease-associated gene sequences in Drosophila melanogaster. Genome Reseach Jun; 11(6):1114-25.

Riano E, Martignoni M, Mancuso G, Cartelli D, Crippa F, Toldo I, Siciliano G, Di Bella D, Taroni F, Bassi MT, Cappelletti G, Rugarli EI. 2009. Pleiotropic effects of spastin on neurite growth depending on expression levels. J Neurochem. Mar;108(5):1277-88

Rodriguez OC, Schaefer AW, Mandato CA, Forscher P, Bement WM, Waterman-Storer CM. 2003. Conserved microtubule-actin interactions in cell movement and morphogenesis. Nat Cell Biol 5(7):599-609.

Santiago C, Bashaw GJ. 2014. Transcription factors and effectors that regulate neuronal morphology. Development 141: 4667-4680.

Satoh, D., D. Sato, T. Tsuyama, M. Saito, H. Ohkura et al., 2008 Spatial control of branching within dendritic arbors by dynein-dependent transport of Rab5-endosomes. Nat Cell Biol 10:1164–1171.

Schaefer MH, Wanker EE, Andrade-Navarro MA. 2012. Evolution and function of CAG/polyglutamine repeats in protein-protein interaction networks. Nucleic Acids Res May;40(10):4273-87.

Schneider CA, Rasband WS, Eliceiri KW. 2012. NIH Image to ImageJ: 25 years of image analysis. Nat Methods Jul;9(7):671-5.

Sears JC, Broihier HT. 2016. FoxO regulates microtubule dynamics and polarity to promote dendrite branching in Drosophila sensory neurons. Dev Biol Oct 1;418(1):40-54.

Sheetz MP, Pfister KK, Bulinski JC, Cotman CW. 1998. Mechanisms of trafficking in axons and dendrites: implications for development and neurodegeneration. Prog Neurobiol 55(6):577-94.

Shin E, Kashiwagi Y, Kuriu T, Iwasaki H, Tanaka T, Koizumi H, Gleeson JG, Okabe S. 2013. Doublecortin-like kinase enhances dendritic remodelling and negatively regulates synapse maturation. Nat Commun. 2013;4:1440.

Siddoway B, Hou H, Xia H. 2014. Molecular mechanisms of homeostatic synaptic downscaling. Neuropharmacology. Mar;78:38-44.

Singhania A, Grueber WB. 2014. Development of the embryonic and larval peripheral nervous system of Drosophila. Wiley Interdiscip Rev Dev Biol. May-Jun;3(3):193-210.

Smith CJ, Watson JD, Spencer WC, O'Brien T, Cha B, Albeg A, Treinin M, Miller DM. 2010. Time-Lapse Imaging and Cell-Specific Expression Profiling Reveal Dynamic Branching and Molecular Determinants of a Multi-Dendritic Nociceptor in C. Elegans. Developmental Biology 345 (1): 18–33.

Song H, Moon M, Choe HK, Han DH, Jang C, Kim A, Cho S, Kim K, Mook-Jung I. 2015. Aβ-induced degradation of BMAL1 and CBP leads to circadian rhythm disruption in Alzheimer's disease. Mol Neurodegener Mar 19;10:13.

Stradal T, Kranewitter W, Winder SJ, Gimona M. 1998. CH domains revisited. FEBS Lett. Jul 17;431(2):134-7.

Sugimura K, Satoh D, Estes P, Crews S, Uemura T. 2004. Development of morphological diversity of dendrites in Drosophila by the BTB-Zinc finger protein Abrupt. Neuron 43(6):809-22.

Sulkowski MJ, Iyer SC, Kurosawa MS, Iyer EP, Cox DN. 2011. Turtle functions downstream of Cut in differentially regulating class specific dendrite morphogenesis in Drosophila. PLoS One 6(7):e22611.

Tang Z, Yu W, Zhang C, Zhao S, Yu Z, Xiao X, Tang R, Xuan Y, Yang W, Hao J, Xu T, Zhang Q, Huang W, Deng W, Guo W. 2016. CREB-binding protein regulates lung cancer growth by targeting MAPK and CPSF4 signaling pathway. Mol Oncol Feb;10(2):317-29.

Tata JR. 2002. Signalling through nuclear receptors. Nat Rev Mol Cell Biol Sep;3(9):702-10.

Tavosanis G. 2014. The cell biology of dendrite differentiation. The Computing Dendrite: From Structure to Function, Springer Series in Computational Neuroscience 11. H. Cuntz et al. (eds).

Tedeschi A, Nguyen T, Puttagunta R, Gaub P, Di Giovanni S. 2009. A p53-CBP/p300 transcription module is required for GAP-43 expression, axon outgrowth, and regeneration. Cell Death Differ Apr;16(4):543-54.

Turner HN, Armengol K, Patel AA, Himmel NJ, Sullivan L, Iyer SC, Bhattacharya S, Iyer EPR, Landry C, Galko MJ, Cox DN. 2016. The TRP Channels Pkd2, NompC, and Trpm Act in Cold-Sensing Neurons to Mediate Unique Aversive Behaviors to Noxious Cold in Drosophila. Curr Biol Dec 5; 26(23):3116-3128.

Valor LM, Viosca J, Lopez-Atalaya JP, Barco A. 2013. Lysine acetyltransferases CBP and p300 as therapeutic targets in cognitive and neurodegenerative disorders. Curr Pharm Des. 19(28):5051-64.

Vandekerckhove J, Weber K. 1978. At least six different actins are expressed in a higher mammal: an analysis based on the amino acid sequence of the amino-terminal tryptic peptide. J Mol Biol. Dec 25;126(4):783-802.

van Dijk J, Rogowski K, Miro J, Lacroix B, Eddé B, Janke C. 2007. A targeted multienzyme mechanism for selective microtubule polyglutamylation. Mol Cell. May 11;26(3):437-48.

Virshup DM, Shenolikar S. 2009. From promiscuity to precision: protein phosphatases get a makeover. Mol Cell. Mar 13;33(5):537-45.

Vo N, Goodman RH. 2001. CREB-binding protein and p300 in transcriptional regulation. J Biol Chem Apr 27;276(17):13505-8.

Wang F, Marshall CB, Ikura M. 2013. Transcriptional/epigenetic regulator CBP/p300 in tumorigenesis: structural and functional versatility in target recognition. Cell Mol Life Sci. Nov;70(21):3989-4008.

Wang X, Zhang MW, Kim JH, Macara AM, Sterne G, Yang T, Ye B. 2015. The Krüppel-like factor Dar1 determines multipolar neuron morphology. J. Neurosci. 35(42):14251-14259.

Wayman GA, Impey S, Marks D, Saneyoshi T, Grant WF, Derkach V, Soderling TR. 2006. Activity-dependent dendritic arborization mediated by CaM-kinase I activation and enhanced CREB-dependent transcription of Wnt-2. Neuron 50(6): 897-909.

Wearne SL, Rodriguez A, Ehlenberger DB, Rocher AB, Hendersion SC, Hof PR. 2005. New Techniques for imaging, digitization and analysis of three-dimensional neural morphology on multiple scales. Neuroscience 136:661-680.

Williams DW, Truman JW. 2005. Cellular mechanisms of dendrite pruning in Drosophila: insights from in vivo time-lapse of remodeling dendritic arborizing sensory neurons. Development 132: 3631–3642.

Wloga D, Dave D, Meagley J, Rogowski K, Jerka-Dziadosz M, Gaertig J. 2010. Hyperglutamylation of tubulin can either stabilize or destabilize microtubules in the same cell. Eukaryot Cell. Jan;9(1):184-93.

Wloga D, Gaertig J. 2010. Post-translational modifications of microtubules. J Cell Sci. Oct 15;123(Pt 20):3447-55.

Won M, Ro H, Park HC, Kim KE, Huh TL, Kim CH, Rhee M. 2006. Dynamic expression patterns of zebrafish 1G5 (1G5z), a calmodulin kinase-like gene in the developing nervous system. Dev Dyn. Mar;235(3):835-42.

Wu JI, Lessard J, Olave IA, Qiu Z, Ghosh A, Graef IA, Crabtree GR. 2007. Regulation of dendritic development by neuron-specific chromatin remodeling complexes. Neuron 56(1): 94-108.

Yamamoto M, Ueda R, Takahashi K, Saigo K, Uemura T. 2006. Control of axonal sprouting and dendrite branching by the Nrg-Ank complex at the neuron-glia interface. Curr Biol 16(16):1678-83.

Yang H, Hou H, Pahng A, Gu H, Nairn AC, Tang YP, Colombo PJ, Xia H. 2015. Protein Phosphatase-1 Inhibitor-2 Is a Novel Memory Suppressor. J Neurosci. Nov 11;35(45):15082-7.

Yang N, MacArthur DG, Gulbin JP, Hahn AG, Beggs AH, Easteal S, North K. 2003. ACTN3 genotype is associated with human elite athletic performance. Am J Hum Genet. Sep;73(3):627-31.

Ye B, Kim JH, Yang L, McLachlan I, Younger S, Jan LY, Jan YN. 2011. Differential regulation of dendritic and axonal development by the novel Krüppel-like factor Dar1. J Neurosci Mar 2;31(9):3309-19.

Zacharogianni M, Kondylis V, Tang Y, Farhan H, Xanthakis D, Fuchs F, Boutros M, Rabouille C. 2011. ERK7 is a negative regulator of protein secretion in response to amino-acid starvation by modulating Sec16 membrane association. EMBO J. Aug 16;30(18):3684-700.

Zhang Q, Gao M, Zhang Y, Song Y, Cheng H, Zhou R. 2016. The germline-enriched Ppp1r36 promotes autophagy. Sci Rep. Apr 21;6:24609.

Zhang Z, Teng CT. 2003. Phosphorylation of Kruppel-like factor 5 (KLF5/IKLF) at the CBP interaction region enhances its transactivation function. Nucleic Acids Res Apr 15;31(8):2196-208.

Zheng Y, Wildonger J, Ye B, Zhang Y, Kita A et al. 2008. Dynein is required for polarized dendritic transport and uniform microtubule orientation in axons. Nat. Cell Biol. 10: 1172–1180.

APPENDIX

Curated list of differentially expressed target genes for *dCBP*-mediated transcriptional repression.

Gene name	**GO Cluster(s)**	**Probable Function (by homology)**	**RNAi lines screened ***
Ppm1	Protein dephosphorylation, protein modification processes	PP2C family, negative regulation of TGF-β signaling and termination of TNF-α-mediated NF-κB activation	B41987 V101257
CG12620	Protein dephosphorylation, protein modification processes, regulation of protein dephosphorylation	protein-phosphatase 1 inhibitor	V39748 V108964
CG6380	Protein dephosphorylation, protein modification processes, regulation of protein dephosphorylation	protein-phosphatase 1 inhibitor	V29950 V100121
CG6036	Protein dephosphorylation, protein modification processes	Downregulation of SMAD2/3:SMAD4 transcriptional activity	B65115 B66318
CG31391	Protein dephosphorylation, protein modification processes, regulation of protein dephosphorylation	protein-phosphatase 1 regulatory subunit	B62891 V107247
Protein phosphatase 1 at 13C	Protein dephosphorylation, protein modification processes	protein-phosphatase 1 catalytic subunit	B32465 V107770
CG32568	Protein dephosphorylation, protein modification processes	Protein-phosphatase 2A regulatory subunit	B38910 B62506
robl62A	Microtubule-based processes	Accessory component of the dynein complex involved in linking dynein to cargo and adapter proteins.	B54813 V104759
Kinesin-like protein at 59C	Microtubule-based processes	Plus end-directed MT-dependent motor, has MT depolymerizing activity	B35596 B64673
Kinesin-like protein at 59D	Microtubule-based processes	Plus end-directed MT-dependent motor, has MT depolymerizing	B35474 B64657

		activity	
CG7716	Microtubule-based processes, cytoskeletal organization	Gamma tubulin	V25526 V104217
Cytoplasmic dynein light chain 2	Microtubule-based processes	Accessory component of the dynein complex involved in linking dynein to cargo and adapter proteins.	V42113 V42114
CG18109	Microtubule-based processes, cytoskeletal organization	Gamma tubulin	B67359 V101222
CG10177	Phosphorylation, protein modification processes	Doublecortin-like kinase	B25945 B55900
Gasket	Phosphorylation, protein modification processes, nervous system development	Constitutively active protein kinase (GSK3β/α homolog)	B64922 V107429 V25641
CG8565	Phosphorylation, protein modification processes	14-3-3 protein binding, upregulation of cyclin-D1 expression via p53 pathway	B55368 B62359
CG16716	Protein modification processes	Polyglutamylase which preferentially modifies β-tubulin	B62488 V106602
CG32238	Protein modification processes	Probable tubulin polyglutamylase	B54016 V109628
Tubulin tyrosine ligase-like 3B	Protein modification processes	Glycylation of α- and β-tubulin and/or component of the Arp2/3 complex regulating actin polymerization	B67791 V104449
Ran-like	Establishment of protein localization	Nuclear protein import and RNA export	B27512 B63003
Actin-related protein 53D	Cytoskeletal organization	Actin filament	B44580 V108369
α actinin 3	Cytoskeletal organization	Actin filament bundle assembly	B26737 V106162
CG17118	Cell morphogenesis	Polyglutamylation of microtubules	B53304 V37623

* B = Bloomington Stock Center, Bloomington Indiana; V = Vienna Drosophila Resource Center, Vienna Austria